1949-07

A study of dynamic forces in aircraft landing gear struts with relation to the optimum angle of suspension

Wood, Harry

St. Paul, Minnesota; University of Minnesota

A STUDY OF DYNAMIC FORCES IN AIRCRAFT LANDING GEAR STRUTS WITH RELATION TO THE OPTIMUM ANGLE OF SUSPENSION

A THESIS

SUBMITTED TO THE GRADUATE FACULTY

of the

UNIVERSITY OF MINNESOTA

by

HARRY WOOD

IN PARTIAL FULFILLMENT OF THE REQUIREMENTS

for the

DEGREE OF MASTER OF SCIENCE IN AERONAUTICAL ENGINEERING

July, 1949

PREFACE

In the more recent years the problems in the design of aircraft landing gear have demanded more attention. One of these problems has been the optimum angle for suspending a landing gear strut in such a manner as to gain the most benefit from the spring system incorporated in the landing gear strut. The study of this optimum angle appears to warrant further analytical and experimental work, and, therefore, was chosen as an appropriate subject for this thesis.

The writer wishes to express his appreciation to his adviser, Professor J. A. Wise, whose suggestions, assistance and criticisms have been most valuable. Thanks are also due to Lieutenant Commander B. V. Turner for his able assistance in experimental work, and to others who assisted in the preparation of this thesis.

TABLE OF CONTENTS

SUMMARY

This report presents the results of a preliminary investigation of the dynamic forces in a Navy type SNJ aircraft landing gear strut with relation to the optimum angle of suspension. Tests were limited to low simulated landing velocities due to insufficiency of the driving power plant. The tests were limited in number due to the malfunctioning of driving unit.

The limited number of tests conducted indicate the optimum angle of suspension to be approximately ten degrees. Test data show that the strut operation is improved by reducing the friction in strut caused by the spin up and spring back drag forces.

It is recommended that test work be conducted to establish the calculable values for the coefficient of friction and load deflection characteristics of aircraft tires during landing impact.

INTRODUCTION

The trend in modern aviation is towards greater weight and faster landing velocities. As these two factors increase the problem of designing a suitable landing gear, yet one which is as light as possible becomes more difficult. One avenue of approach is to suspend the landing gear strut at an angle such that the drag force caused by the initial impact does not have an adverse effect upon the spring properties of the strut and the stresses produced by these drag forces are not greater than those stresses which are induced when the landing strut snaps back after the spin-up of the wheel.

Since very little is known about the optimum angle for suspending a landing gear strut, an investigation of this subject was carried on in the Landing Gear Pit at the University of Minnesota's Rosemount Research Center.

In this investigation the drag forces, axial strut forces, tire deflections, and the relative motion between wheel and the suspension point of the strut were measured. The strut and wheel of a Navy SNJ type aircraft were used in this test work.

This investigation is limited in scope due to the following factors: (1) time available for testing after completion of test equipment; (2) low simulated landing velocities due to output of power plant; (3) insufficient data

on coefficient of friction of rubber under rolling impact loads; (4) insufficient data on sliding friction in oleo of strut; (5) inability to measure sinking velocity accurately.

APPARATUS AND INSTRUMENTS

A major part of the time devoted to this thesis was spent in the construction of suitable equipment for drop testing landing gear struts under simulated landing conditions. A ten foot diameter flywheel from a Corliss steam engine was mounted on pedestals in a pit located in Building 717A at Rosemount Research Center. The flywheel was driven by the use of an automobile engine through a reduction gear. This arrangement is shown in Figure 1 below.

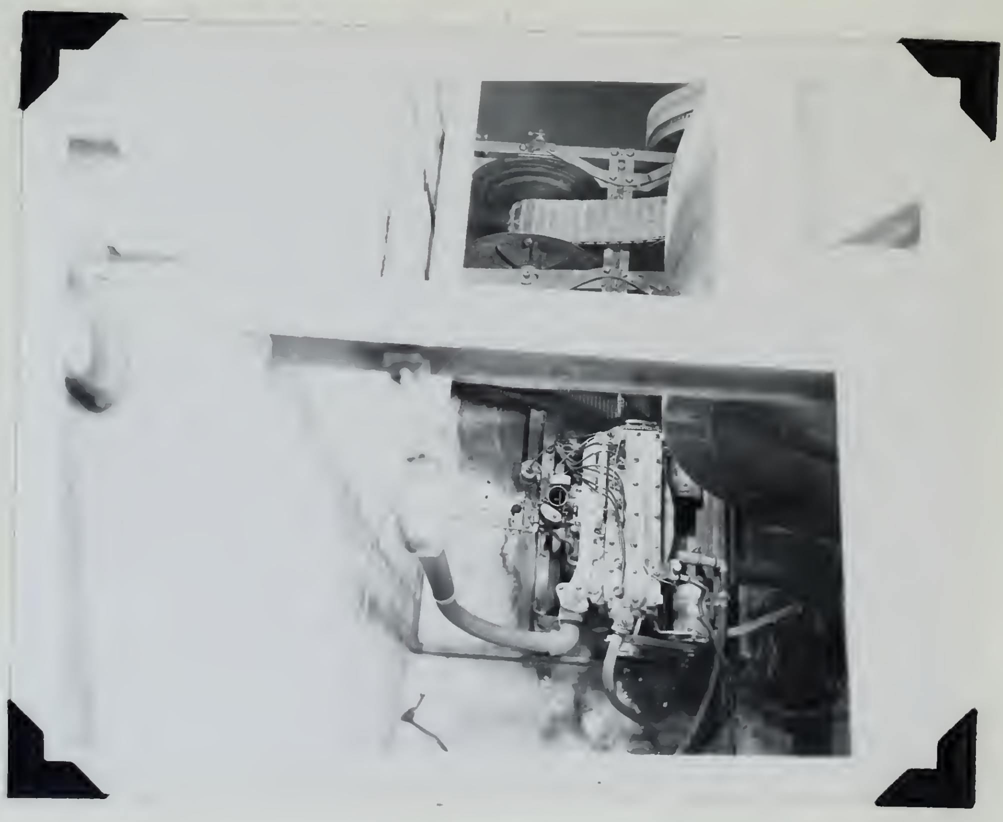

FIGURE 1

A great deal of trouble was encountered in obtaining the desired peripheral velocity on the flywheel due to frictional type pulleys on the reduction gear. The peripheral velocity of the flywheel simulated the ground speed of an aircraft while landing.

A platform mounted upon a pivot arm was used for varying simulated aircraft weights and its free falling velocity was used to simulate aircraft sinking velocities. An adjustable linking arm hung from the platform and into this fitted a linkage box through which the landing gear strut was suspended. This linkage box could be rotated in the plane of simulated landing direction for the purpose of varying the angle of inclination of the landing gear strut. These parts are shown assembled with strut and wheel in Figures 2 and 3 on the following pages.

The strut used in these tests is the standard landing gear strut used on Navy type SNJ aircraft. A standard 27 inch aircraft wheel and tire were mounted on the strut. The strut was serviced and inflated as directed in SNJ maintenance manual. The strut was suspended from the linkage box by means of a standard SNJ strut suspension bracket.

Strain gauges of the C-1 type were mounted at opposite points on the front and rear of the landing gear fork to obtain drag forces. The same type strain gauges were mounted at opposite points on the inside and outside of the landing gear fork to measure the axial forces in the strut.

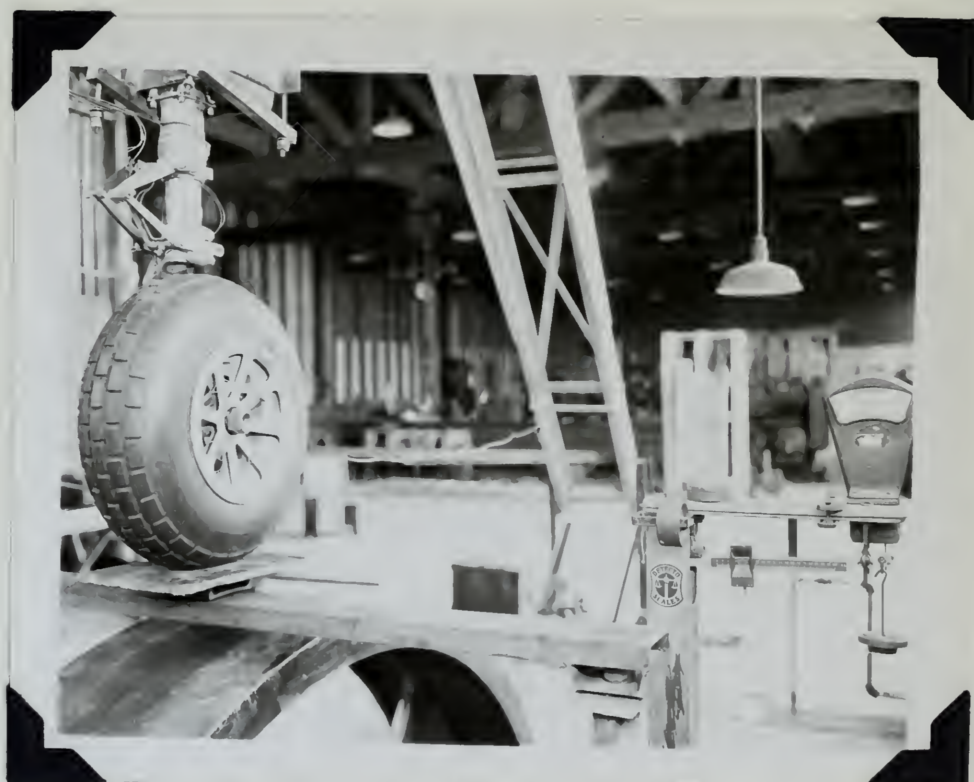

FIGURE 2

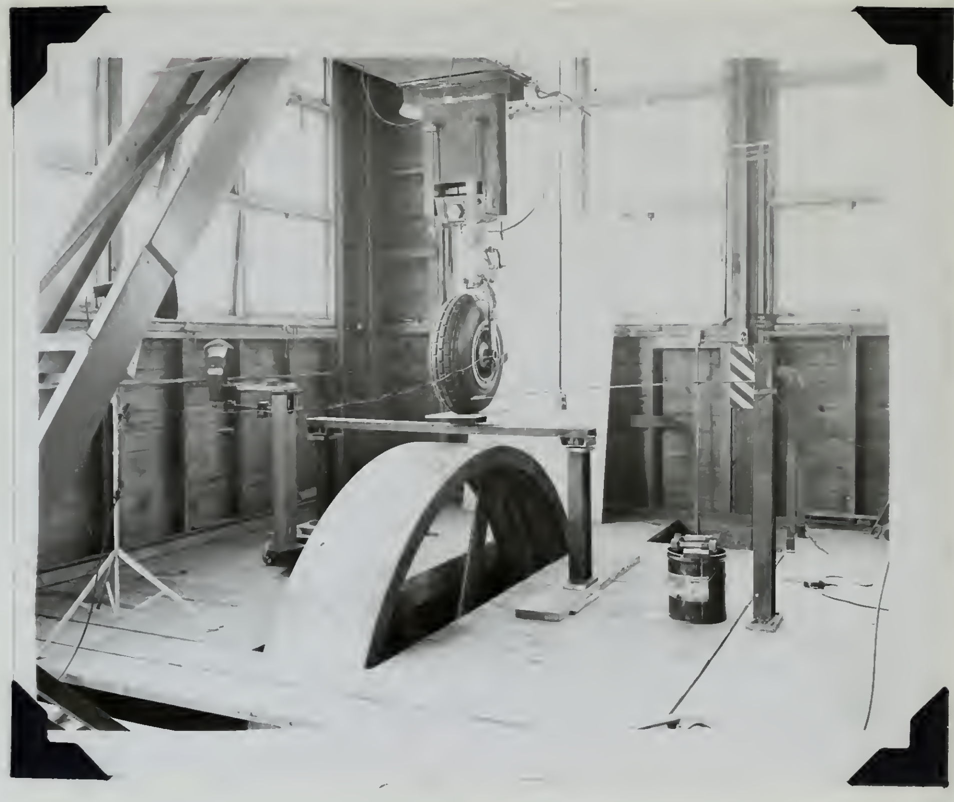

FIGURE 3

Tire deflections were obtained by mounting C-1 type strain gauges on a cantilever beam. The end of the cantilever beam was displaced by the vertical motion of the bottom of the axle, and since the displacement of the axle was due to the tire deflection a reading of tire deflection could be obtained from the cantilever deflection. Oleo deflections were measured by the use of a potentiometer which was rotated by a scissors attachment between the stationary and movable part of the oleo. Mountings of the above instruments are shown in Figure 4 on the following page. Readings from the above instruments were recorded by the use of strain analyzers to which Brush oscilloscopes were attached for recording purposes.

The weighing system was composed of a beam with two knife edges, one of which rested on a fixed upright while the other rested on an upright which in turn was supported by ordinary platform scales. The tire, bearing the simulated aircraft weight, was supported on a third knife edge at a point near the middle of the beam. This lever system is shown in Figure 3 also.

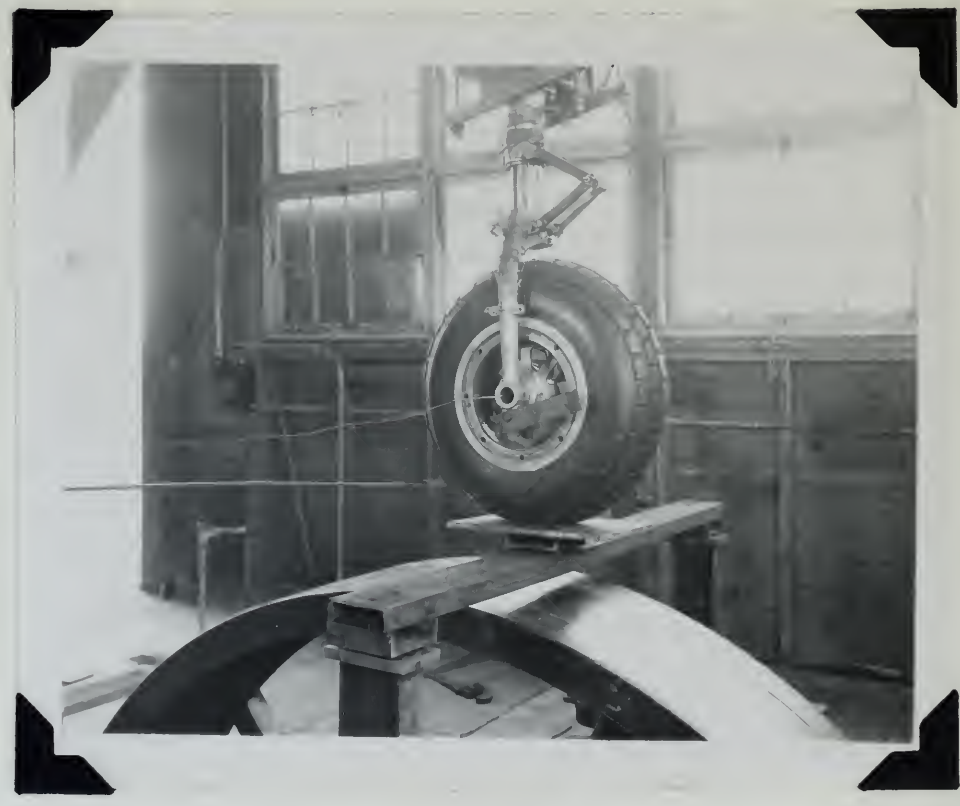

FIGURE 4

TESTING PROCEDURE

The linkage box and pivot arm platform were calibrated first for strut angle inclination and points of suspension from pivot arm platform. These calibration points were taken so that at each test angle of the strut tested the aircraft wheel would rest on top of the large flywheel. These calibrations were made with the oleo fully compressed.

Prior to each day's test work it was necessary to balance the strain analyzers used in recording the strains and deflections of the strain gauges and potentiometer. After balancing the strain analyzers the displacement curves of the Brush oscilloscopes were calibrated.

The displacement due to axial force in the landing gear fork was calibrated first. This was accomplished by turning the strut to a vertical position, allowing the weight of the structure to rest on tire, obtaining this weight from the weighing system and noting the deflection of the Brush oscilloscope. It was possible to make this type calibration due to the fact that the center line of the aircraft wheel was displaced a small amount from the center line of the landing gear fork. This small amount of eccentricity produced a given bending moment for each different vertical force acting on the aircraft wheel. This vertical force acting on the aircraft wheel was the axial force in the landing gear fork.

The potentiometer for measuring oleo displacements was calibrated at the same time. This calibration was accomplished by plotting oleo displacement in inches versus Brush oscilloscope displacement in millimeters.

The cantilever strain gauges were calibrated by noting the deflection of the Brush oscilloscope in millimeters due to a measured tire deflection in inches.

The drag force strain gauges were calibrated by applying a drag force of known magnitude to the strut and noting the deflection of the Brush oscilloscope in millimeters.

Flywheel revolutions were measured by the use of a stroboscope. The peripheral velocity was computed in feet per second and used as simulated landing velocity. Sinking velocities were attained by dropping the landing gear and pivot arm from a vertical height. These heights were calculated for the velocities which would be attained by a freely falling body. Dropping was made possible by a quick release mechanism attached to the pivot arm.

Having completed these calculations the strut was set at the angle desired for testing. Tests were begun by bringing the flywheel up to the speed required to simulate the desired landing speed. The aircraft wheel was raised by the pivot arm to the height required to attain the sinking velocity desired at the time of contact between tire and

revolving flywheel. The Brush oscilloscopes were turned on and the landing gear dropped on the turning flywheel. The Brush oscilloscopes printed a record of drag force, axial force, tire deflection and oleo deflection versus time. Another test at the same strut angle could be run as soon as the pivot arm and aircraft wheel were raised to the height required to attain desired sinking velocity. The elapsed time between such tests was approximately two minutes.

TEST DATA AND RESULTS

The results of these tests are shown in Figures 5A through 30B. Figure 5A is a plot of the spring characteristic of the tire used on the strut during testing, while Figure 5B is a plot of the spring characteristic exhibited by the oleo when under static loads.

Figure 6 is a calibration curve for the purpose of converting the data from the potentiometer, as recorded by the Brush recorder, into oleo deflection in inches.

Test data as recorded by Brush oscilloscopes is shown in Figures 7 through 29. In these figures, the horizontal axis represents time, each five millimeters representing four one-hundredths of a second. The top curve in each figure represents the drag force perpendicular to the strut and is marked drag. The second curve in each figure represents the axial force acting on the strut. The third curve in each figure represents the tire deflection and is labeled cantilever, to correspond with the method used to measure the tire deflections. These curves may be read directly by using the calibration on each figure. The bottom curve in each figure represents the compression of the oleo and is labeled potentiometer. This curve must be read by reference to Figure 6. The sum of the two bottom curves gives the displacement of the mass above the

oleo. Zero time and displacement are indicated by the intersection of the heavy dark line with the curve.

Tests with the strut in a vertical position and at ten degrees inclination show the drag and axial forces and the tire displacements to be approximately straight line variation for a short time.

The presence of friction in the moving part of the oleo is clearly indicated in all figures. This friction is indicated by the change in slope of the potentiometer curve which indicates a slower rate of displacement of the oleo when the curve flattens out. By comparing the curves indicating drag forces with the potentiometer curves indicating oleo compression, it can be seen that the maximum drag forces correspond with a decrease in rate of displacement of the oleo. This indicates that the friction is due to the bending moment forces caused by the drag loads. An angle of inclination of ten degrees shows less pronounced frictional effects on the operation of the oleo than do other angles of suspension.

Figures 7 through 14 indicate quite clearly that drag forces, axial forces, and tire deflections increase with an increase in sinking velocity.

All of the curves indicate that the drag forces, axial forces and tire deflections damp out quite rapidly. The

potentiometer curve indicates that the wheel does not have a vibration period of its own, but vibrates as a unit with the wheel.

Figure 30A shows a plot of drag forces versus angle of inclination of the strut. Curve A is the maximum spin up drag forces encountered with a sinking velocity of two feet per second; curve B represents these drag forces when the sinking velocity is five feet per second. Drag forces for sinking velocities of three and four feet per second will fall between curves A and B. Curve C represents the maximum snap back drag forces encountered with a sinking velocity of two feet per second; curve D represents these drag forces for a sinking velocity of five feet per second. The snap back drag forces for sinking velocities of three and four feet per second will fall between curves C and D. The point of intersection of the spin up and snap back curves for the same sinking velocities indicates that these two forces are equal. This indicates the optimum angle of suspension to produce equal bending moments in the strut when the wheel spins up and then snaps back. The small number of test points available for plotting these curves indicate this optimum angle to be approximately ten degrees.

Figure 30B is a plot of axial force versus angle of inclination. The minimum points on these curves indicate

the optimum angle of inclination for minimum axial force to be approximately twenty-four degrees.

The bending moments due to the drag forces produce quite high stresses in the strut; these stresses are decreased very little by the axial forces since they are small; hence, the optimum angle for producing minimum drag forces is the important angle to consider in design.

These tests are not conclusive as to optimum angle for suspending a landing gear strut. Other tests should be conducted in which the landing velocity and gross weight of the SNJ type aircraft are more nearly simulated. Tests should also be carried out with the strut suspended at a greater number of angles.

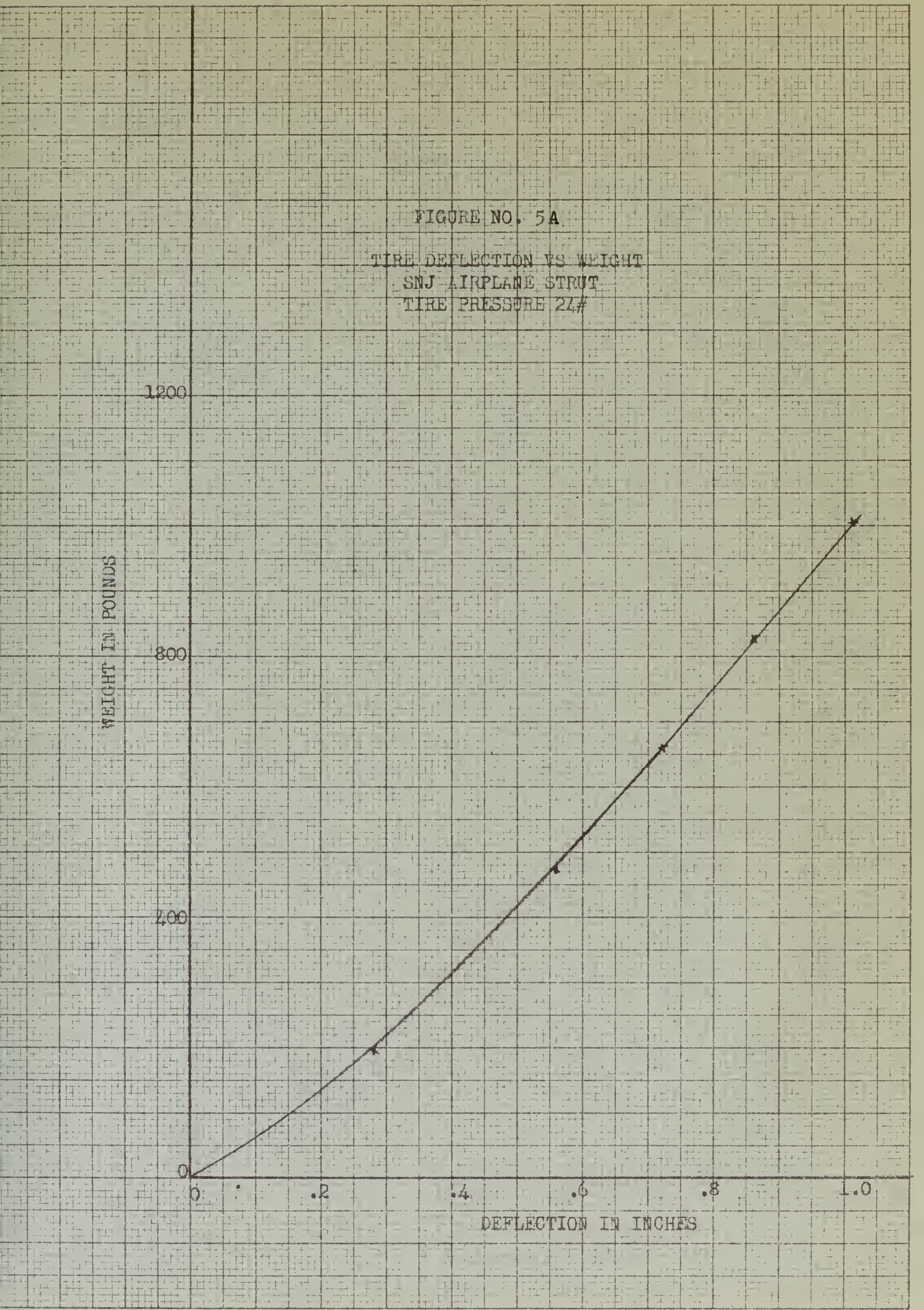
FIGURE NO. 5A
TIRE DEFLECTION VS WEIGHT
SNJ AIRPLANE STRUT
TIRE PRESSURE 24#
WEIGHT IN POUNDS
1200
800
400
0
0
.2
.4
.6
.8
1.0
DEFLECTION IN INCHES

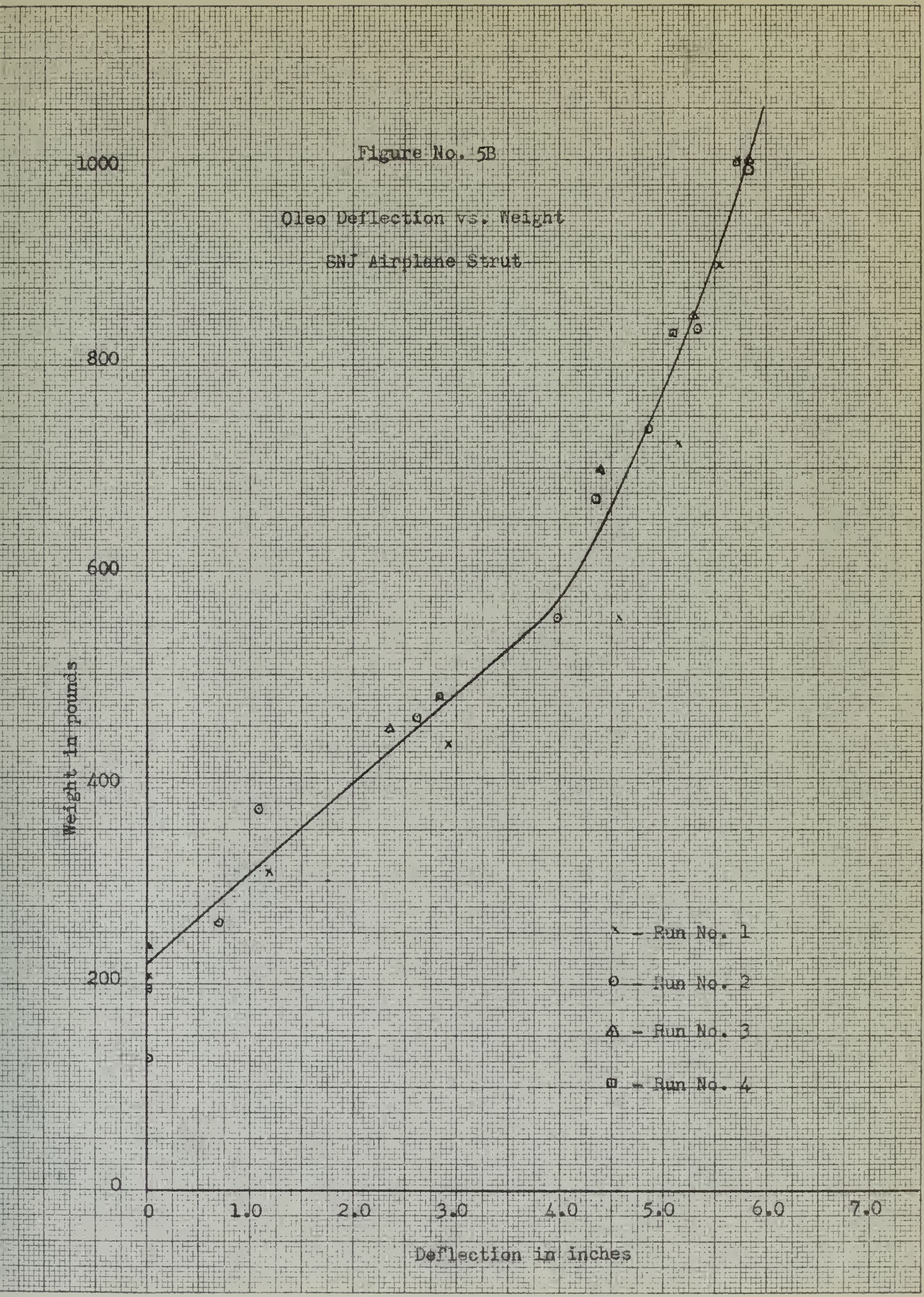
Figure No. 5B
Oleo Deflection vs. Weight
SNJ Airplane Strut
Weight in pounds
0
200
400
600
800
1000
0
1.0
2.0
3.0
4.0
5.0
6.0
7.0
Deflection in inches
x - Run No. 1
o - Run No. 2
△ - Run No. 3
□ - Run No. 4

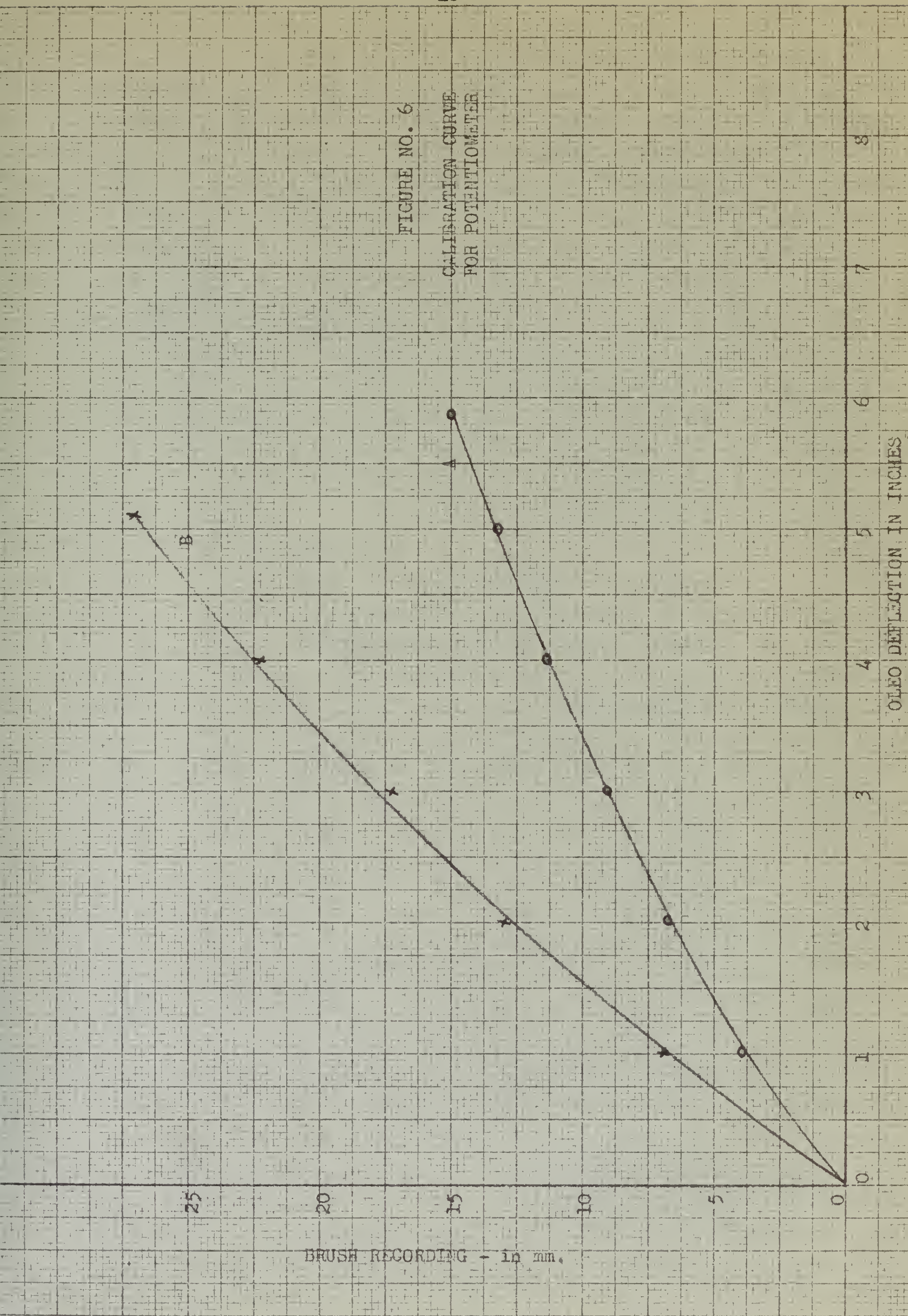
FIGURE NO. 6
CALIBRATION CURVE
FOR POTENTIOMETER
A
B
OLEO DEFLECTION IN INCHES
0
1
2
3
4
5
6
7
8
BRUSH RECORDING - in mm.
0
5
10
15
20
25

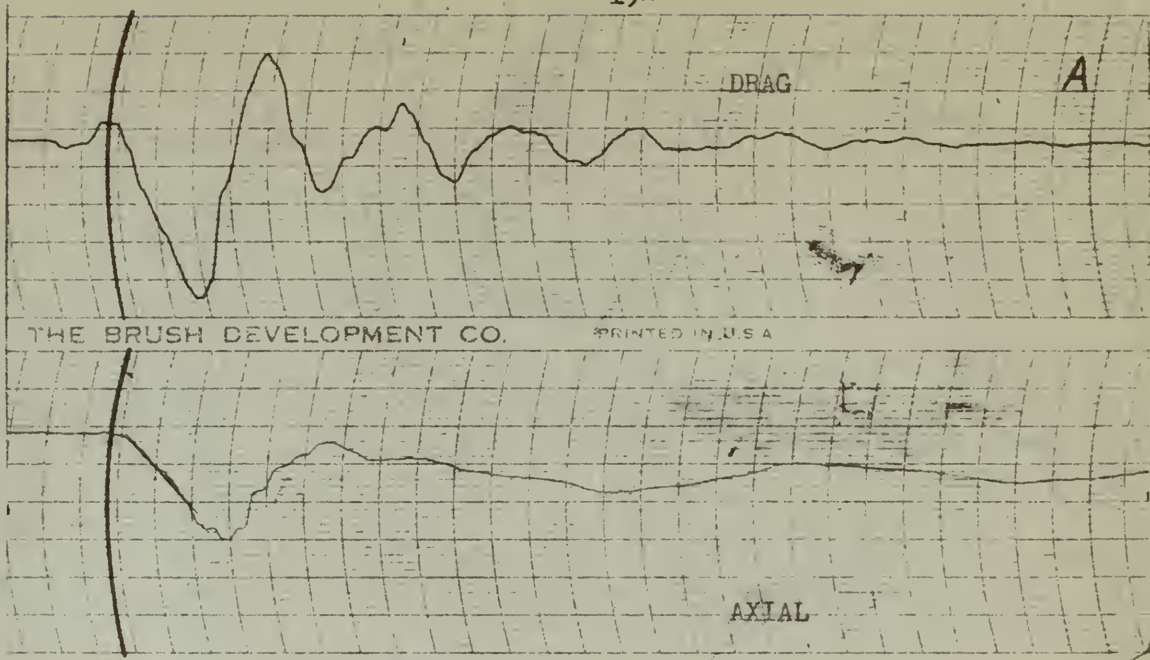

CALIBRATION:

DRAG - 2 mm. = 128#
AXIAL - 2.5 mm. = 462#
CANTILEVER - 1 mm. = .325 in.
POTENTIOMETER - REFER CURVE "A" FIG. 6

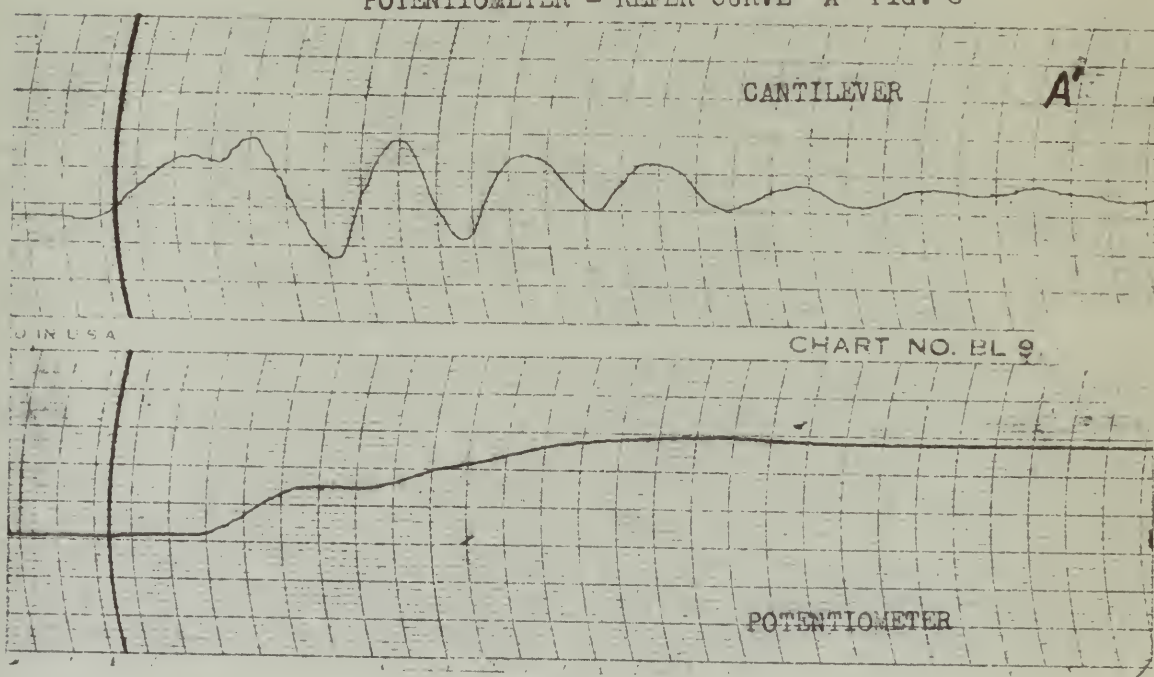

FIG. 7

DATE: 7/9/49
STRUT ANGLE 0°
WEIGHT 1060#

TIRE PRESSURE 24#
LANDING VELOCITY 52.5 F.P.S.
DROPPING VELOCITY 2 F.P.S.
PAPER SPEED 125 mm./sec.

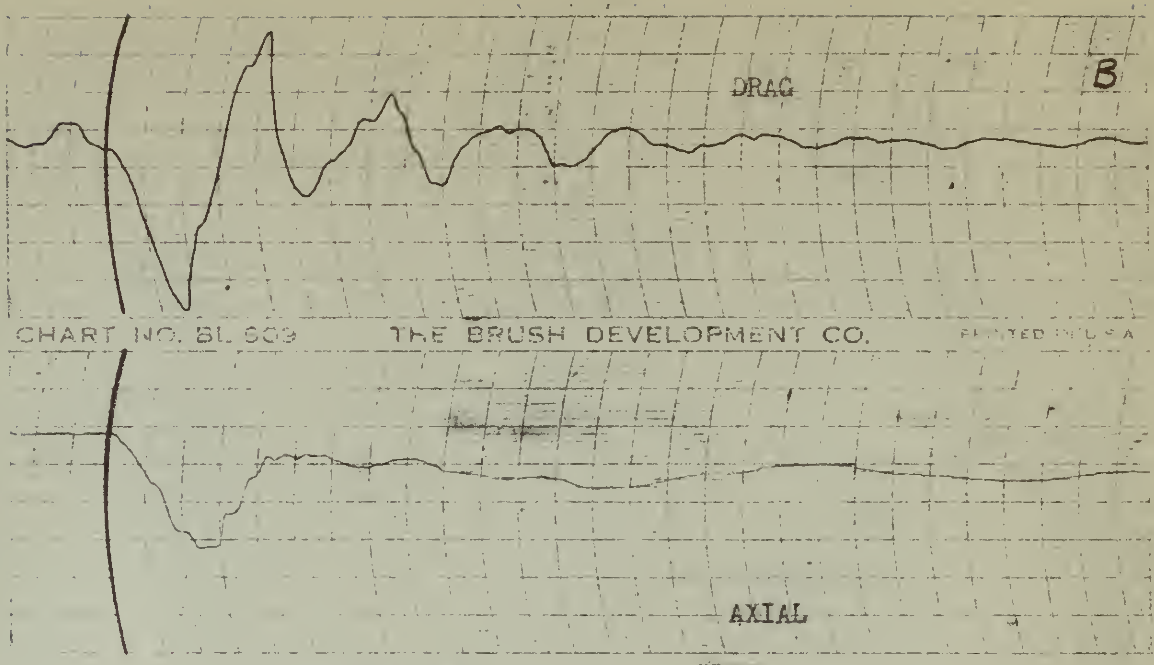

CALIBRATION:
DRAG - 2 mm. = 128#
AXIAL - 2.5mm. = 462#
CANTILEVER - 1 mm. = .325 in.
POTENTIOMETER - REFER CURVE "A" FIG. 6

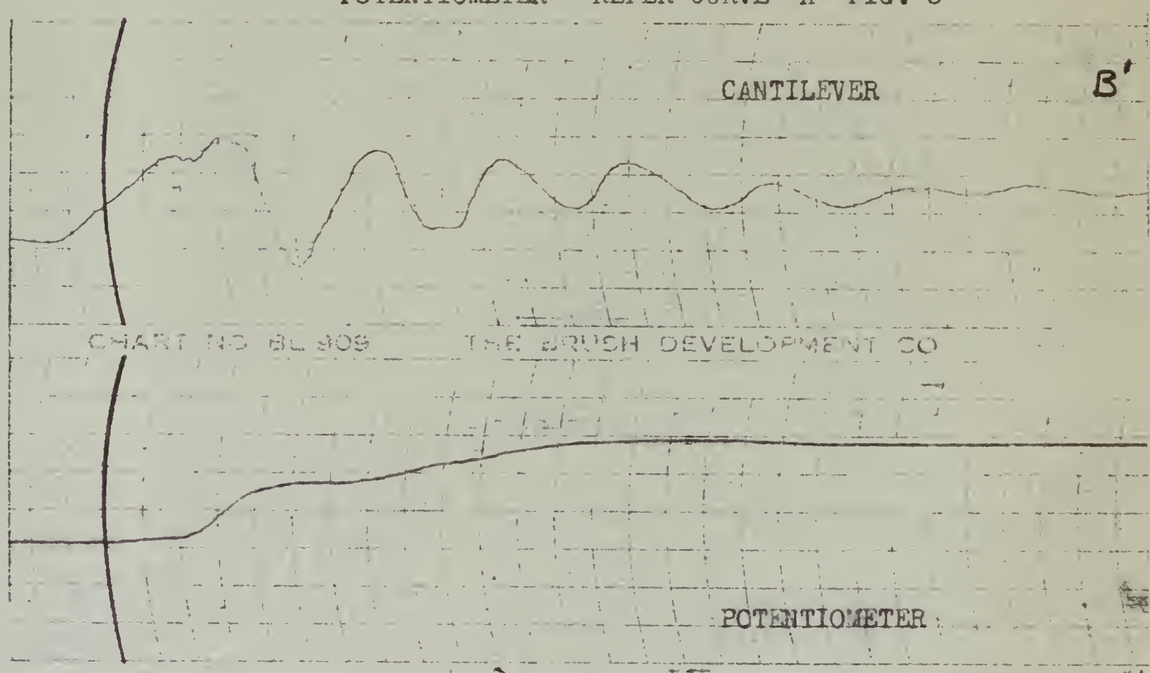

FIG. 8

DATE: 7/9/49
STRUT ANGLE 0°
WEIGHT 1060#

TIRE PRESSURE 24#
LANDING VELOCITY 52.5 F.P.S.
DROPPING VELOCITY 3 F.P.S.
PAPER SPEED 125 mm./sec.

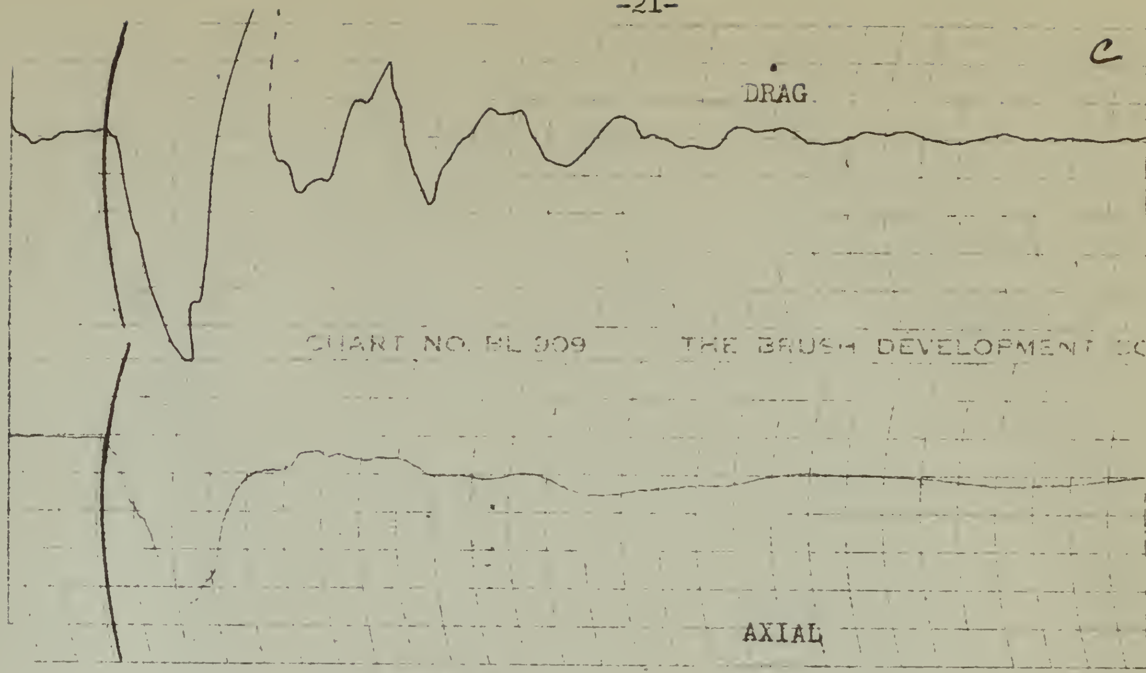

CALIBRATION:
DRAG - 2 mm. = 128#
AXIAL - 2.5 mm. = 462#
CANTILEVER - 1 mm. = .325 in.
POTENTIOMETER - REFER CURVE "A" FIG. 6

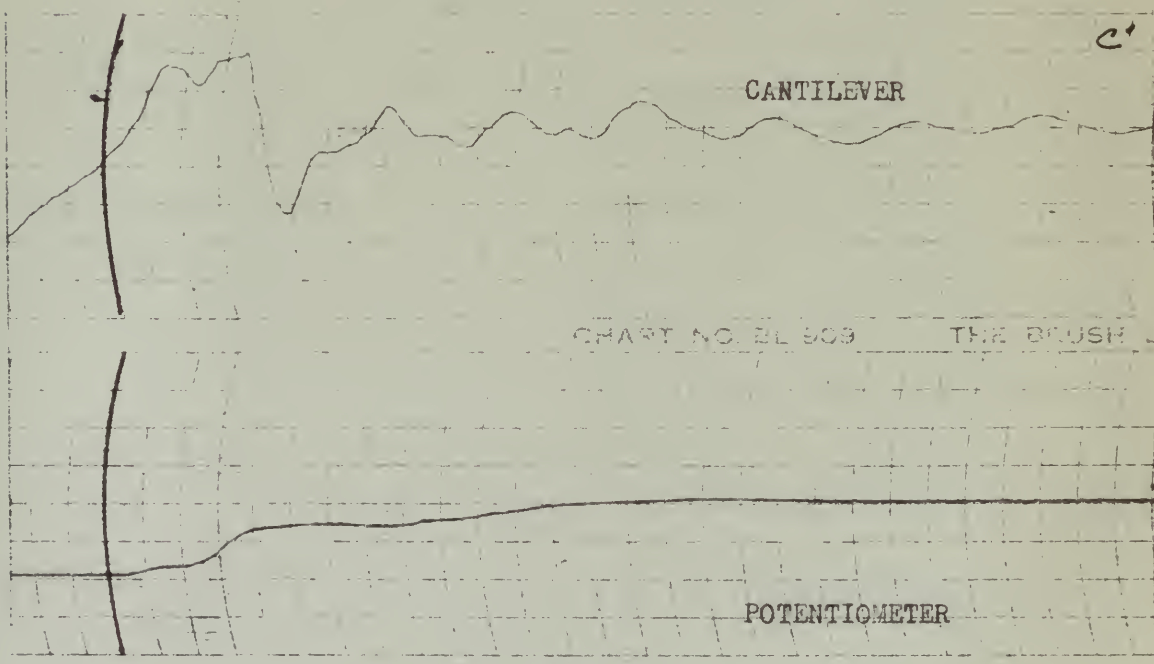

FIG. 9

DATE: 7/9/49
STRUT ANGLE 0°
WEIGHT 1060#

TIRE PRESSURE 24#
LANDING VELOCITY 52.5 F.P.S.
DROPPING VELOCITY 4 F.P.S.
PAPER SPEED 125 mm./sec.

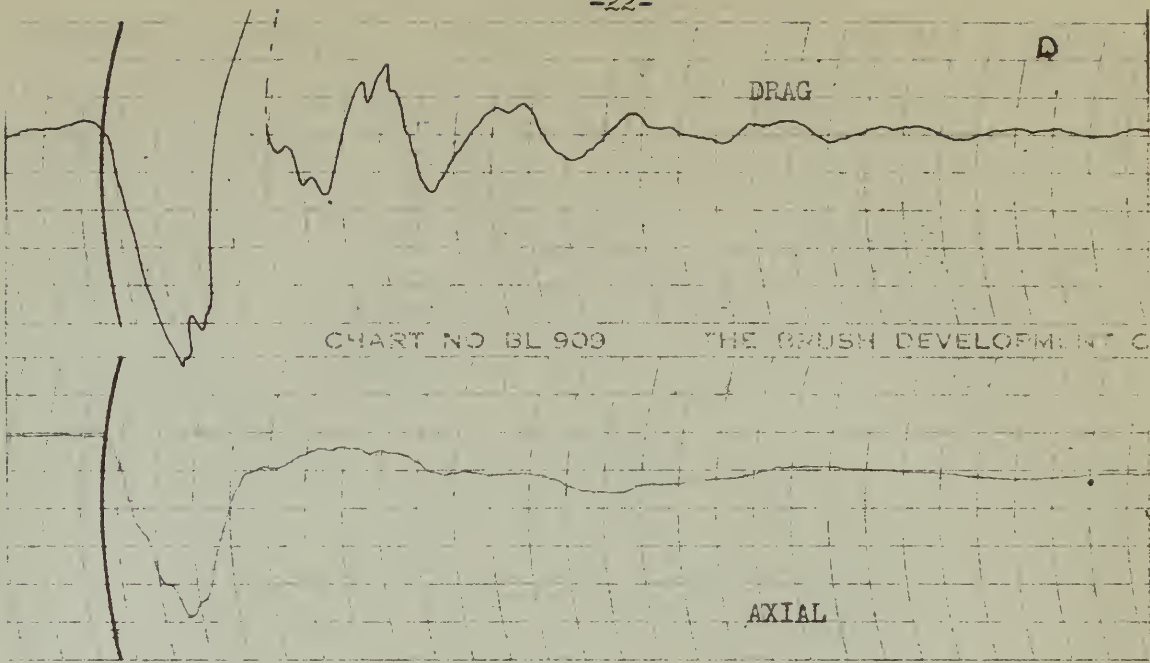

CALIBRATION:

DRAG - 2 mm.= 128#
AXIAL - 2.5 mm.= 462#
CANTILEVER - 1 mm.= .325 in.
POTENTIOMETER - REFER CURVE "A" FIG. 6

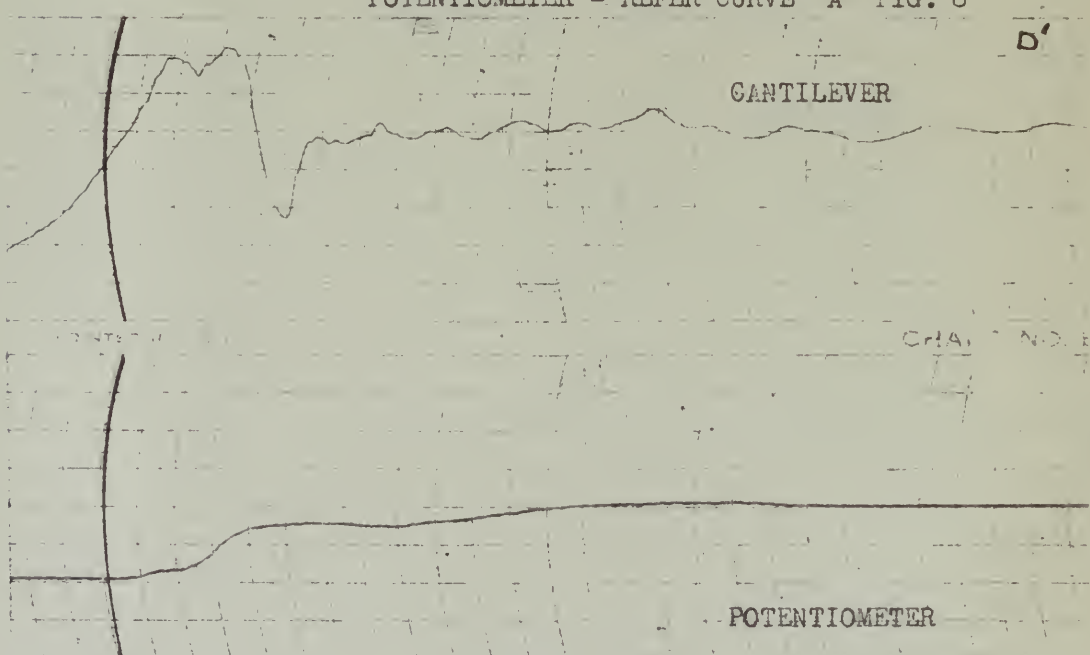

FIG. 10

DATE: 7/9/49
STRUT ANGLE 0°
WEIGHT 1060#

TIRE PRESSURE 24#
LANDING VELOCITY 52.5 F.P.S.
DROPPING VELOCITY 5 F.P.S.
PAPER SPEED 125 mm./sec.

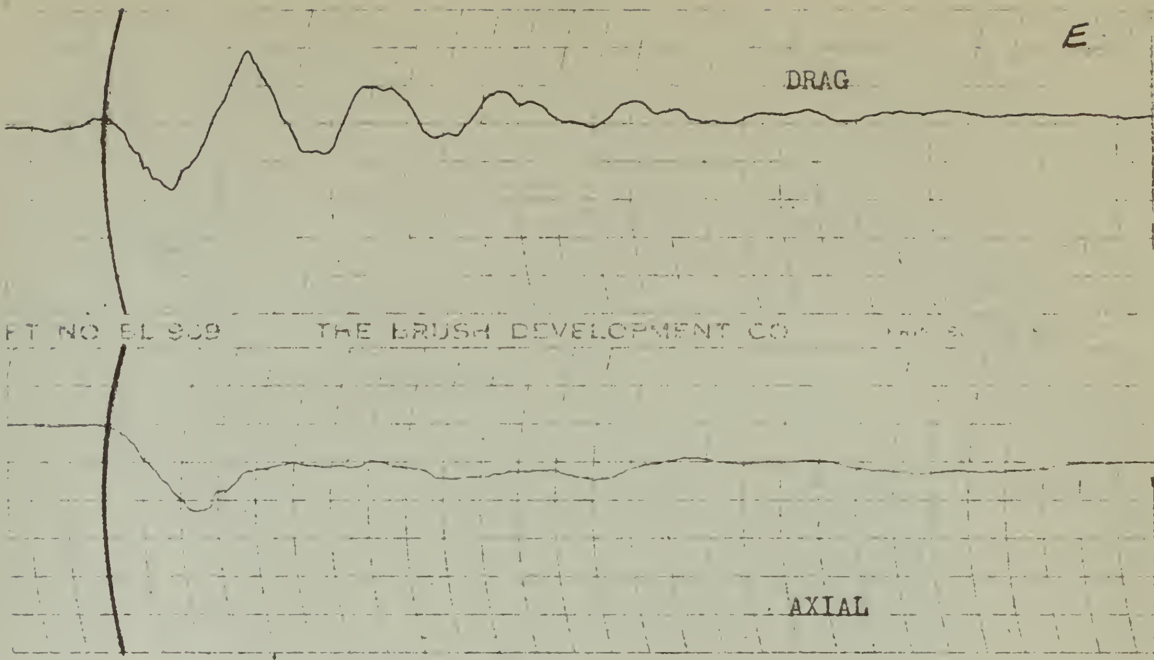

CALIBRATION:
DRAG - 2 mm. = 220#
AXIAL - 5 mm. = 930#
CANTILEVER - 1 mm. = .375 in.
POTENTIOMETER - REFER CURVE "B" FIG. 6

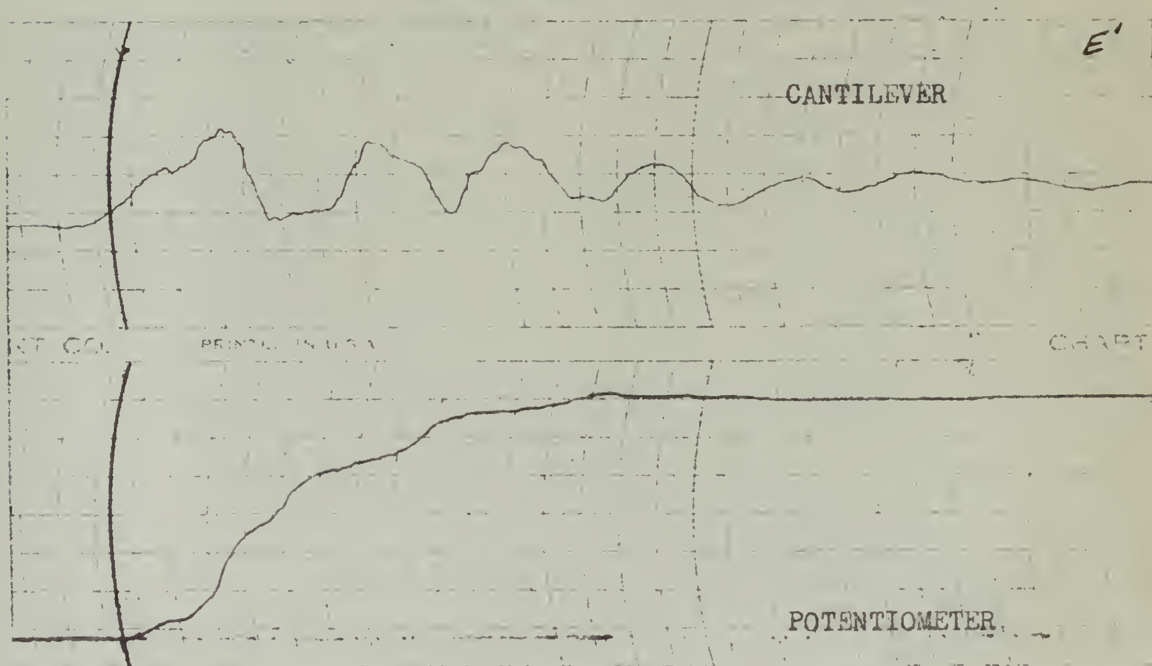

FIG. 11

DATE: 7/10/49
STRUT ANGLE 10°
WEIGHT 1060#

TIRE PRESSURE 24#
LANDING VELOCITY 55 F.P.S.
DROPPING VELOCITY 2 F.P.S.
PAPER SPEED 125 mm./sec.

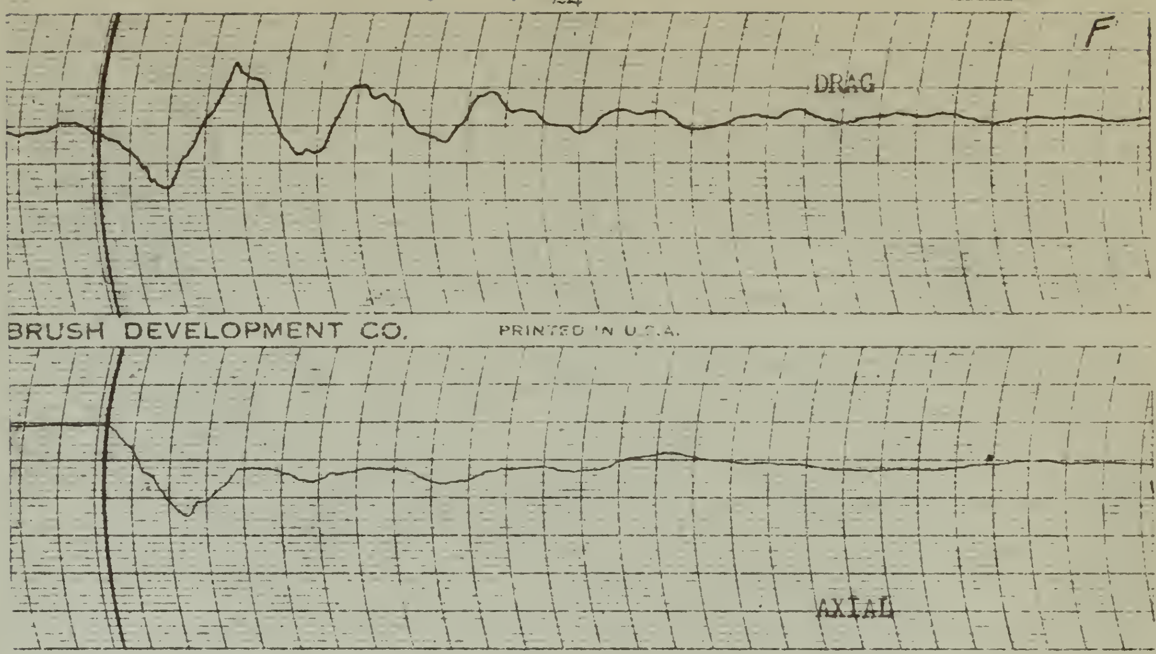

CALIBRATION:
DRAG - 2 mm. = 220#
AXIAL - 5 mm. = 930#
CANTILEVER - 1 mm. = .375 in.
POTENTIOMETER - REFER CURVE "B" FIG. 6

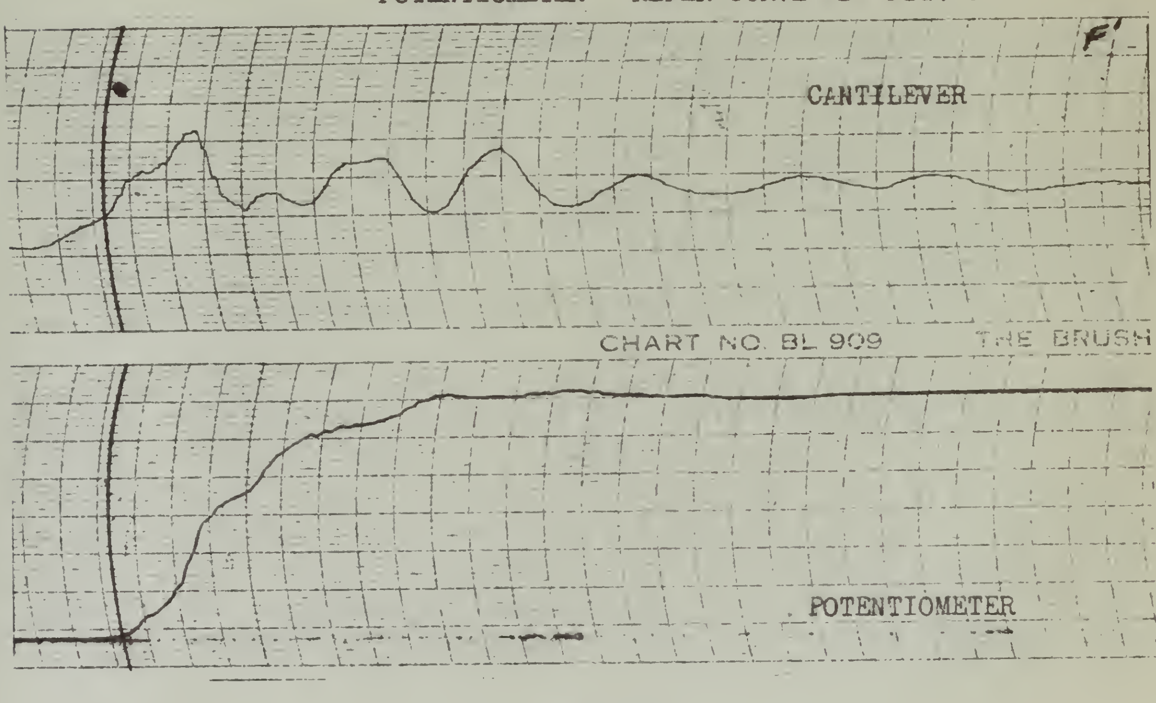

FIG. 12

DATE: 7/10/49
STRUT ANGLE 10°
WEIGHT 1060#

TIRE PRESSURE 24#
LANDING VELOCITY 55 F.P.S.
DROPPING VELOCITY 3 F.P.S.
PAPER SPEED 125 mm./sec.

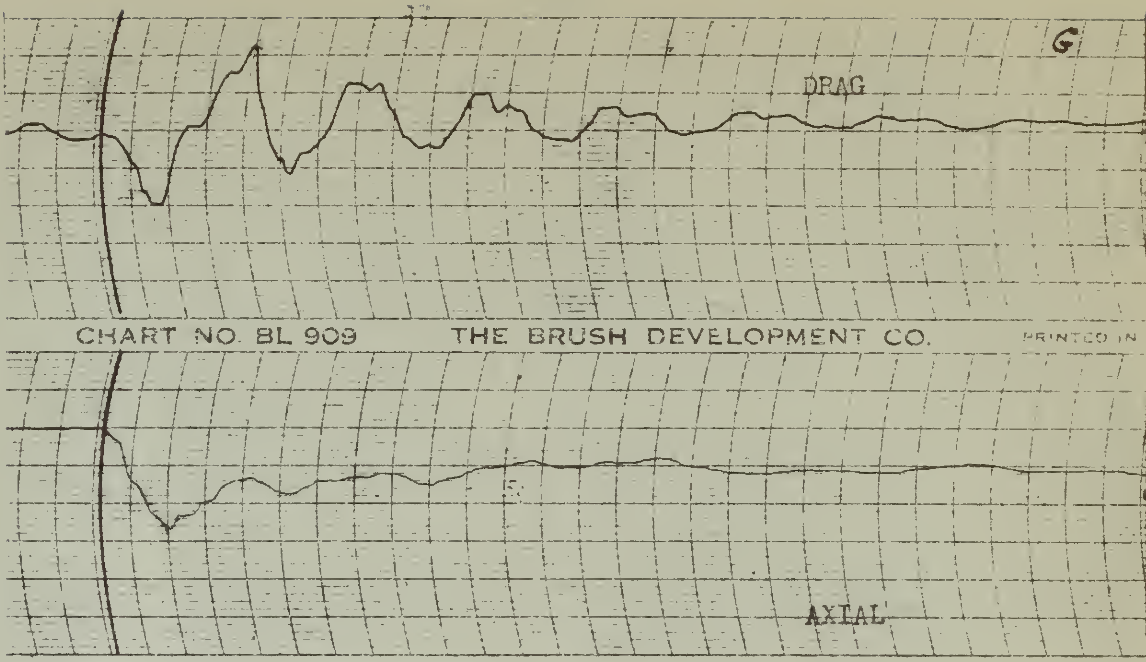

CALIBRATION:
DRAG - 2 mm. = 220#
AXIAL - 5 mm. = 930#
CANTILEVER - 1 mm. = .375 in.
POTENTIOMETER - REFER CURVE "B" FIG. 6

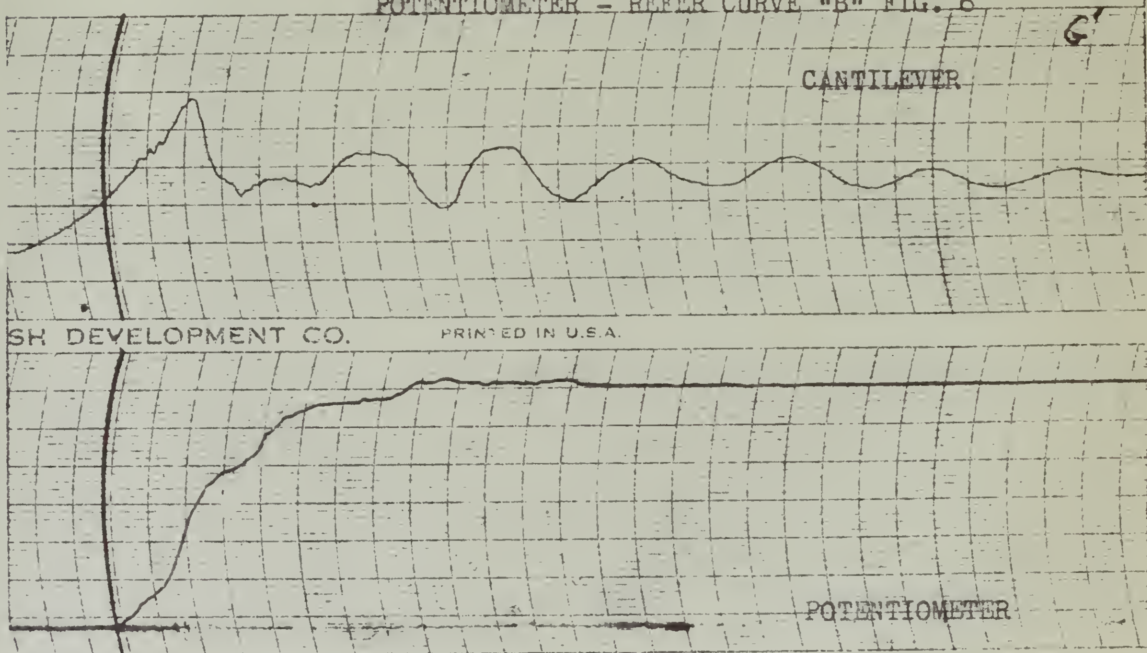

FIG. 13

DATE: 7/10/49
STRUT ANGLE 10°
WEIGHT 1060#

TIRE PRESSURE 24#
LANDING VELOCITY 55 F.P.S.
DROPPING VELOCITY 4 F.P.S.
PAPER SPEED 125 mm./sec.

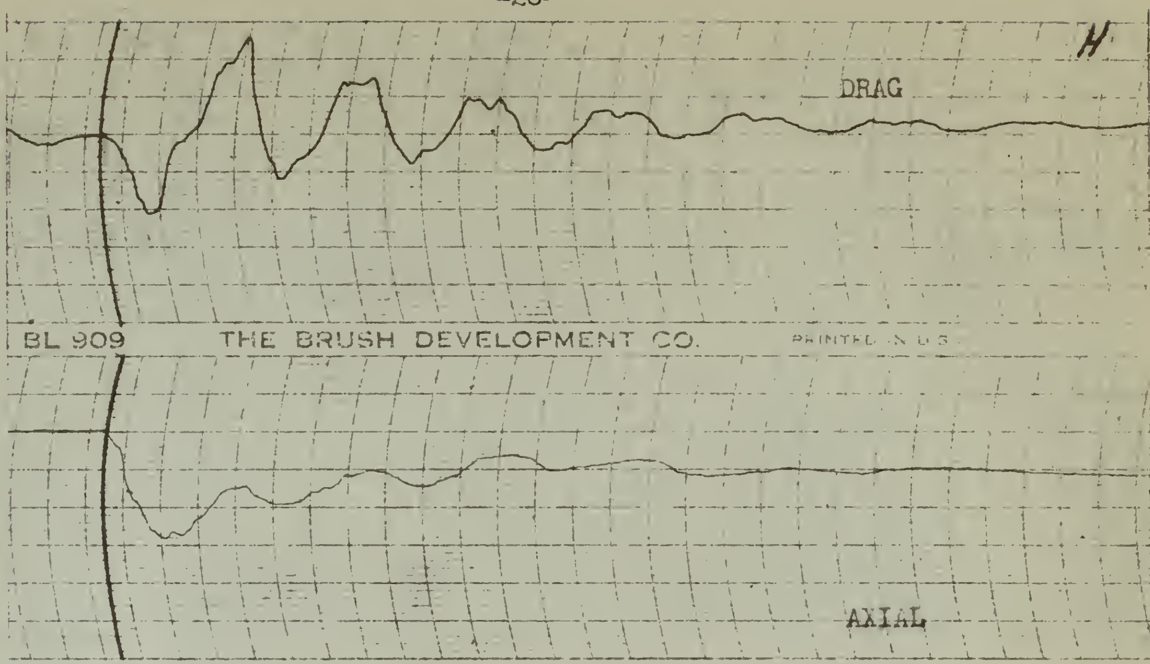

CALIBRATION:
DRAG - 2 mm. = 220#
AXIAL - 5 mm. = 930#
CANTILEVER - 1 mm. = .375 in.
POTENTIOMETER - REFER CURVE "B" FIG. 6

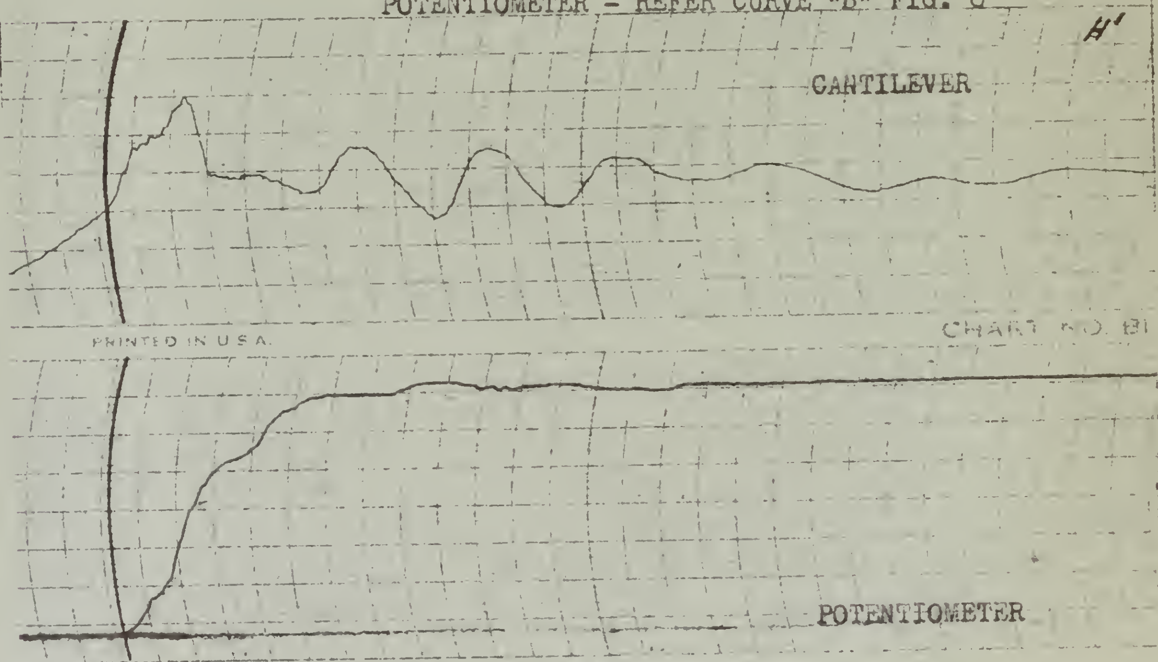

FIG. 14

DATE: 7/10/49
STRUT ANGLE 10°
WEIGHT 1060#

TIRE PRESSURE 24#
LANDING VELOCITY 55 F.P.S.
DROPPING VELOCITY 5 F.P.S.
PAPER SPEED 125 mm./sec.

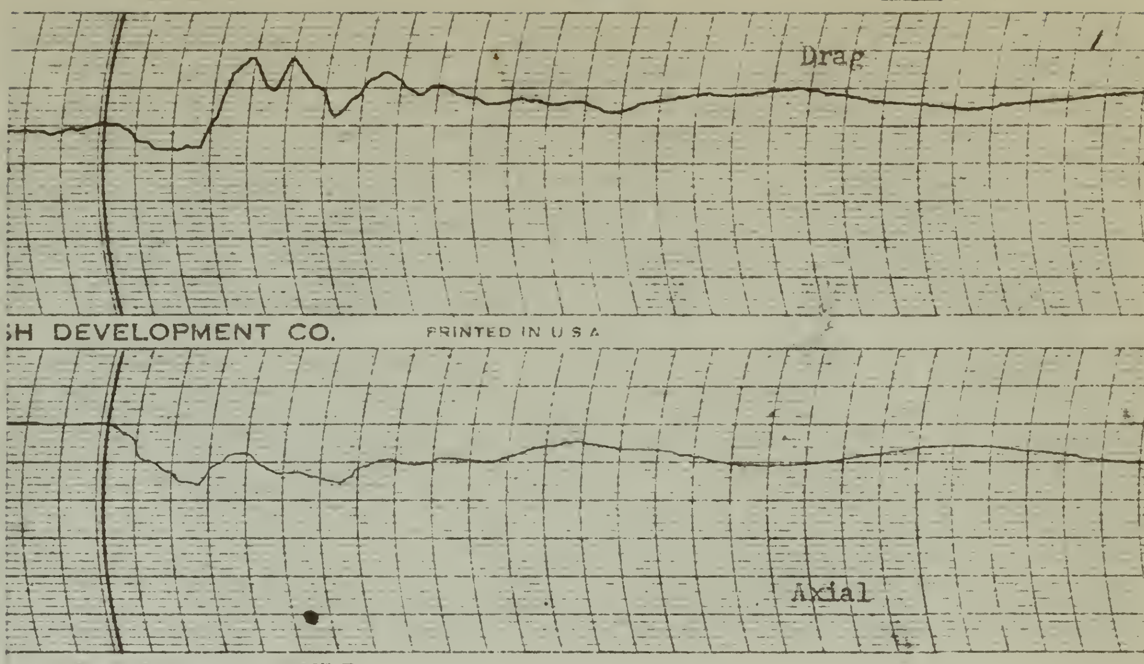

Calibration:

Drag - 1 mm - 220#
Axial - 5 mm = 930#

Cantilever - 1 mm - .375"
Potentiometer - Refer to Fig. No. 6 Curve B

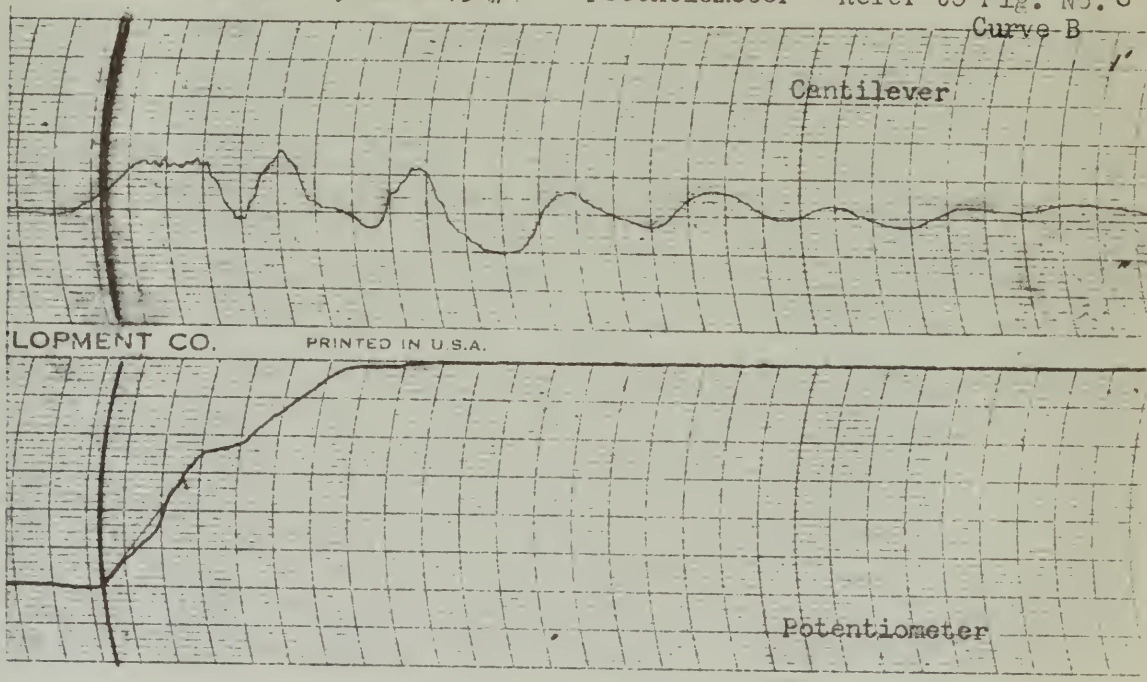

Fig. No. 15

Date: 7/10/49
Strut Angle - 24°
Weight - 1060#
Paper Speed 125 mm/sec

Tire Pressure - 24#
Landing Velocity - 58 FPS
Dropping Velocity - 2 FPS.

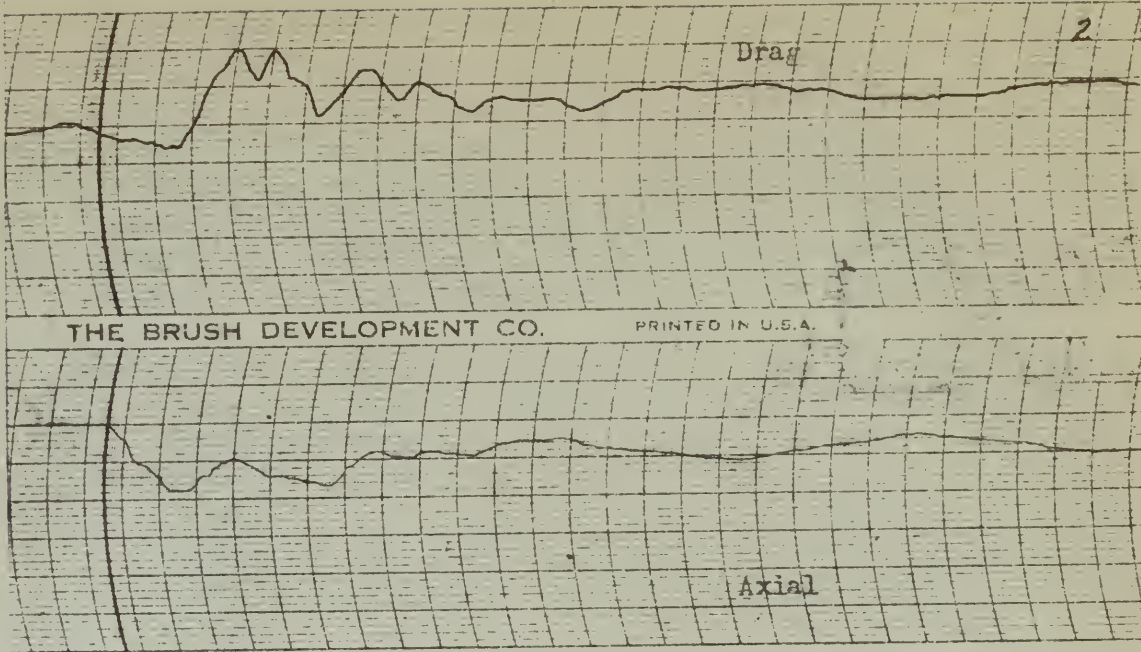

Calibration:

Drag - 1 mm = 220#
Axial - 5 mm = 930#

Cantilever - 1 mm = .375"
Potentiometer - Refer to Fig. No. 6. Curve B

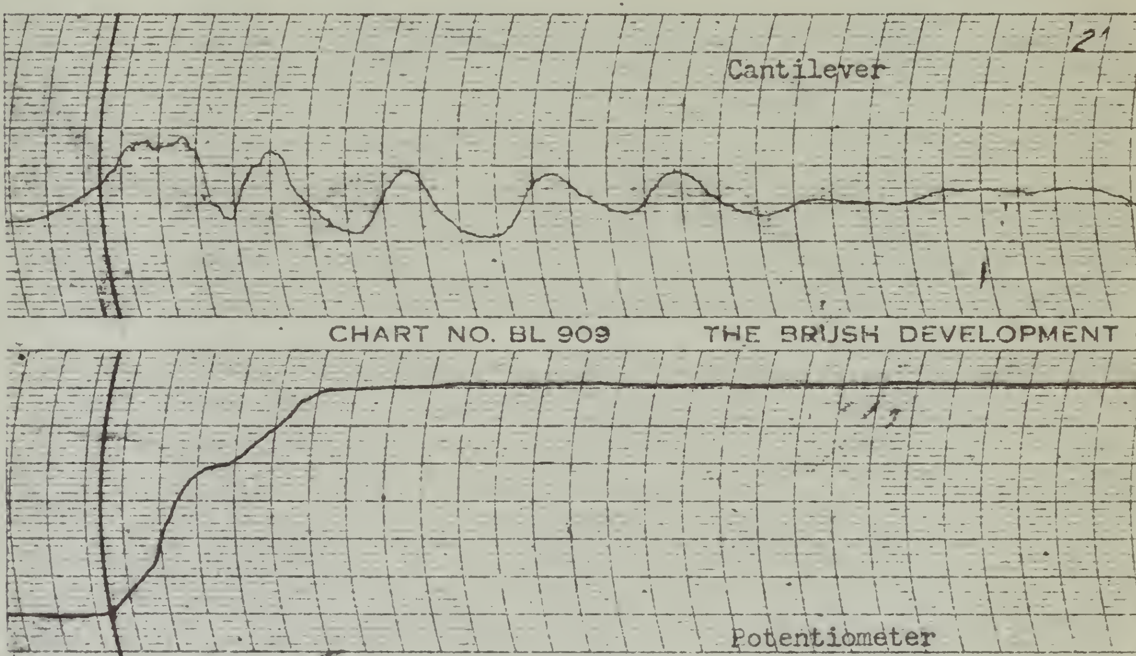

Fig. No. 16

Date: 7/10/49
Strut Angle - 24°
Weight - 1060#
Paper Speed 125 mm/sec

Tire Pressure - 24#
Landing Velocity - 58 FPS
Dropping Velocity - 3 FPS.

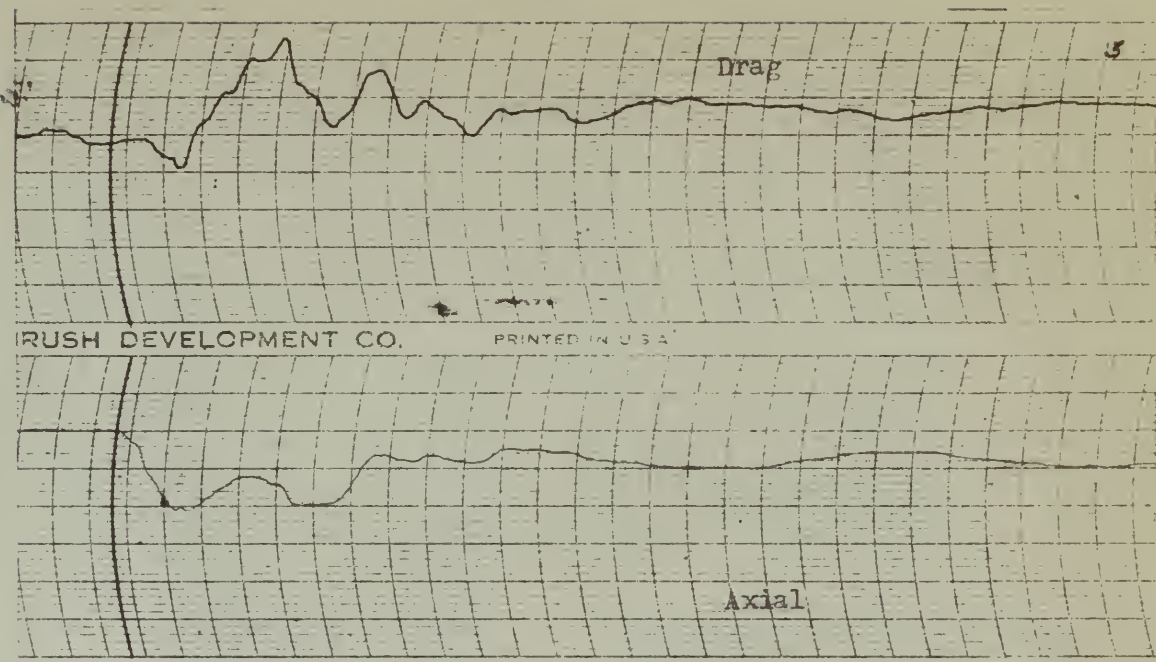

Calibration:
Drag - 1 mm = 220#
Axial - 5 mm = 930#
Cantilever ,- 1 mm = .375"
Potentiometer - Refer to Fig. 6 Curve B

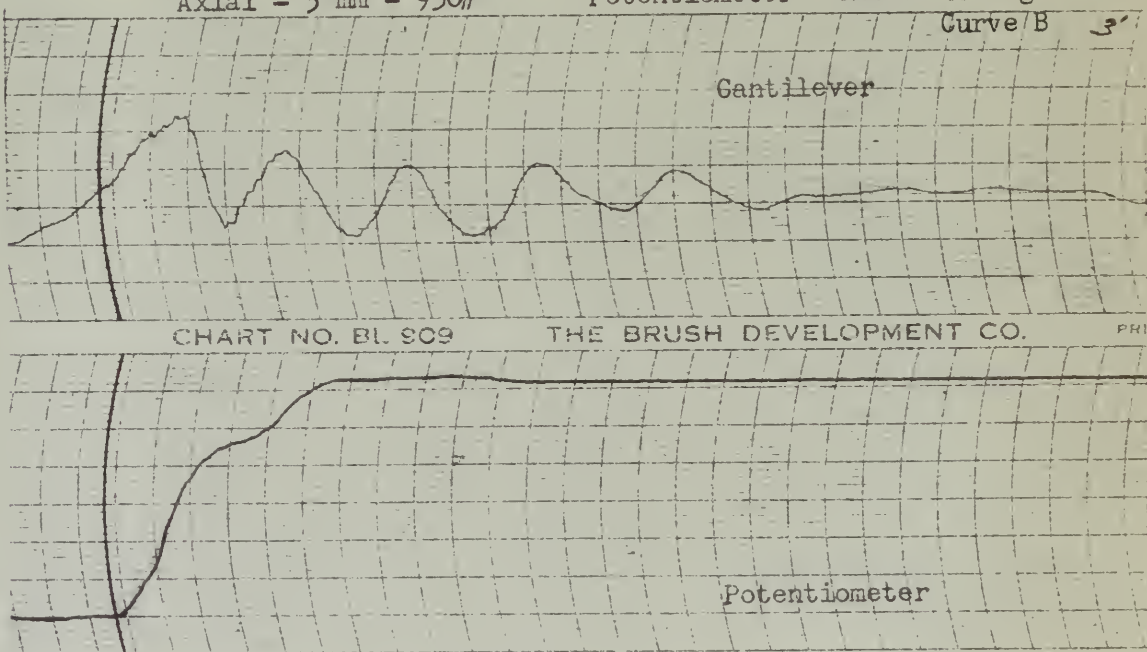

Fig. No. 17

Date: 7/10/49
Strut Angle - 24°
Weight - 1060#
Brush Speed 125 mm/sec

Tire Pressure - 24#
Landing Velocity - 58 FPS
Dropping Velocity - 4 FPS.

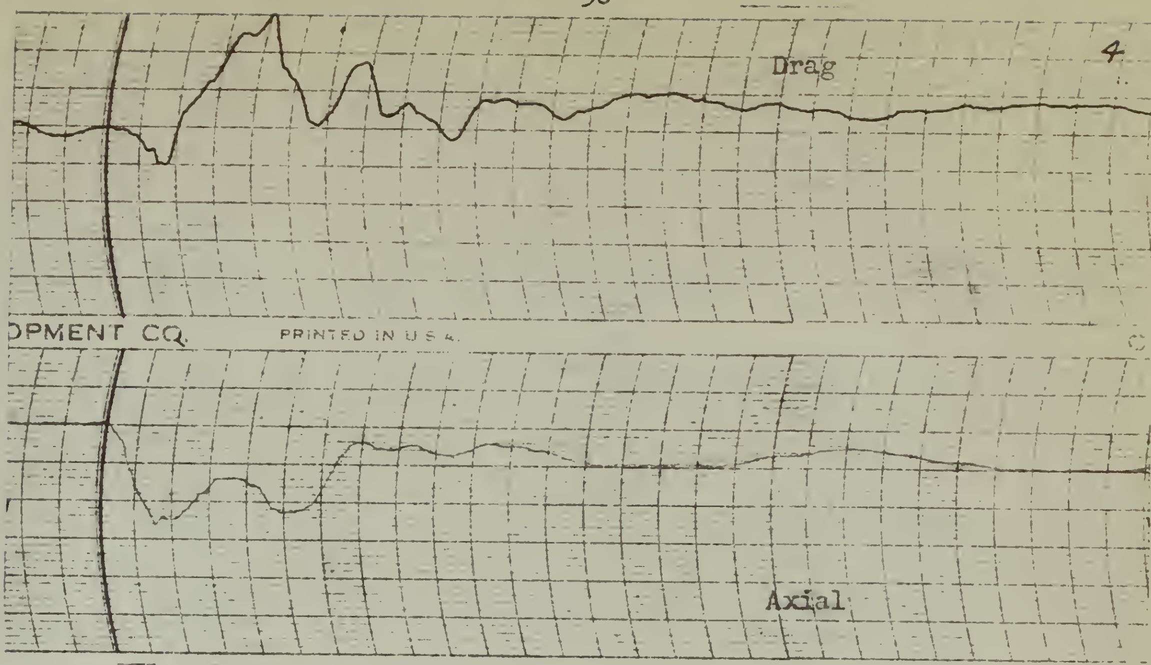

Calibration:

Drag - 1 mm = 220#
Axial - 5 mm = 930#

Cantilever - 1 mm = .375"
Potentiometer - Refer to Fig. 6 Curve B

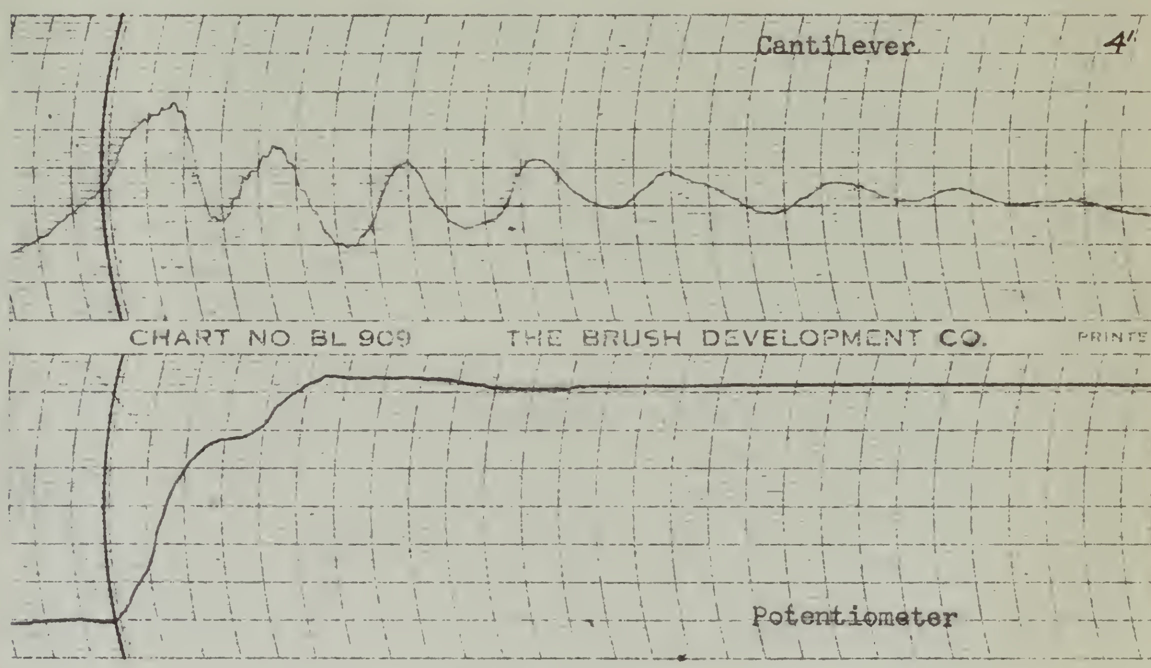

Fig. No. 18

Date: 7/10/49
Strut Angle - 24°
Weight - 1060#
Brush Speed 125 mm/sec.

Tire Pressure - 24#
Landing Velocity - 58 FPS.
Dropping Velocity - 5 FPS.

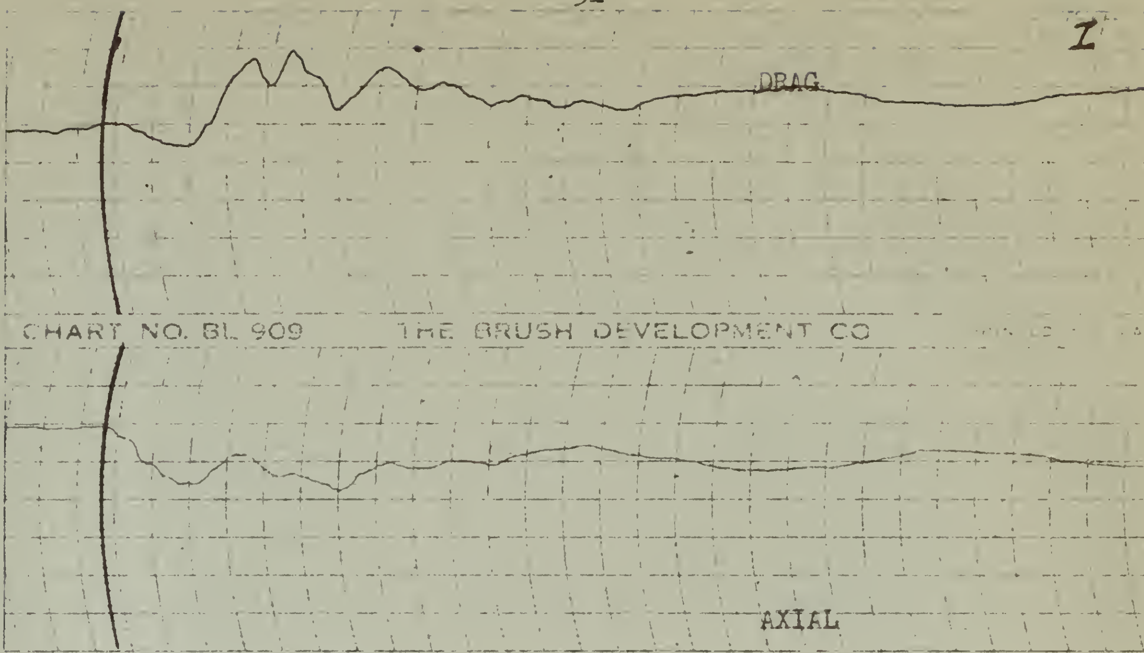

CALIBRATION:

DRAG	- 1 mm. = 220#	
AXIAL	- 5 mm. = 930#	
CANTILEVER	- 1 mm. = .375 in.	
POTENTIOMETER	- REFER CURVE "B" FIG. 6	

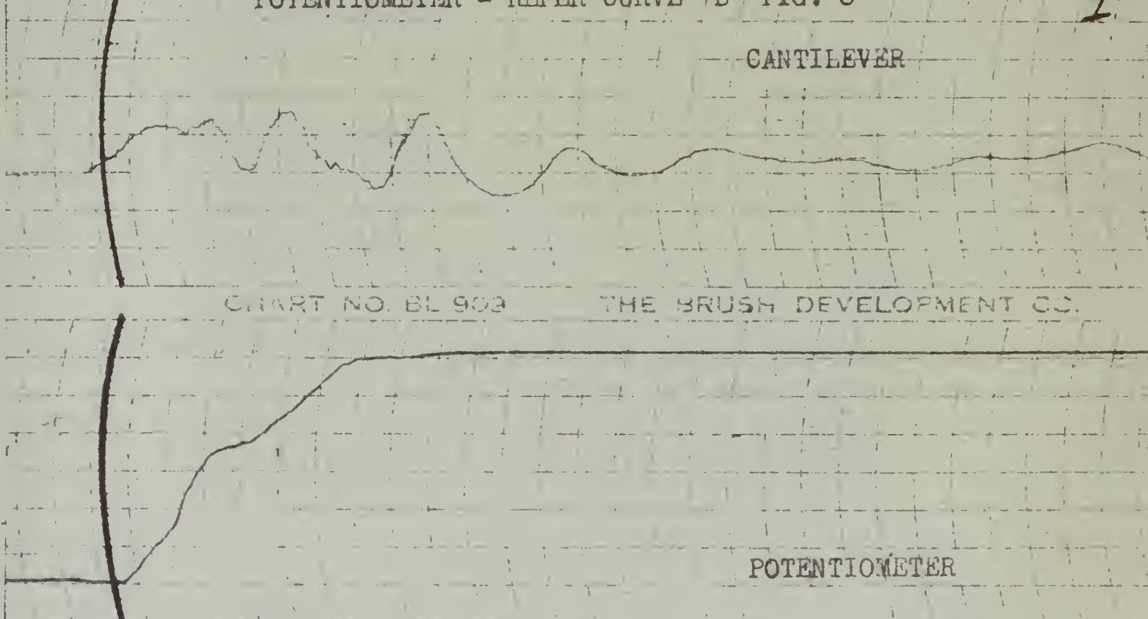

FIG. 19

DATE: 7/10/49
STRUT ANGLE 26°
WEIGHT 1060#

TIRE PRESSURE 24#
LANDING VELOCITY 60 F.P.S.
DROPPING VELOCITY 2 F.P.S.
PAPER SPEED 125 mm./sec.

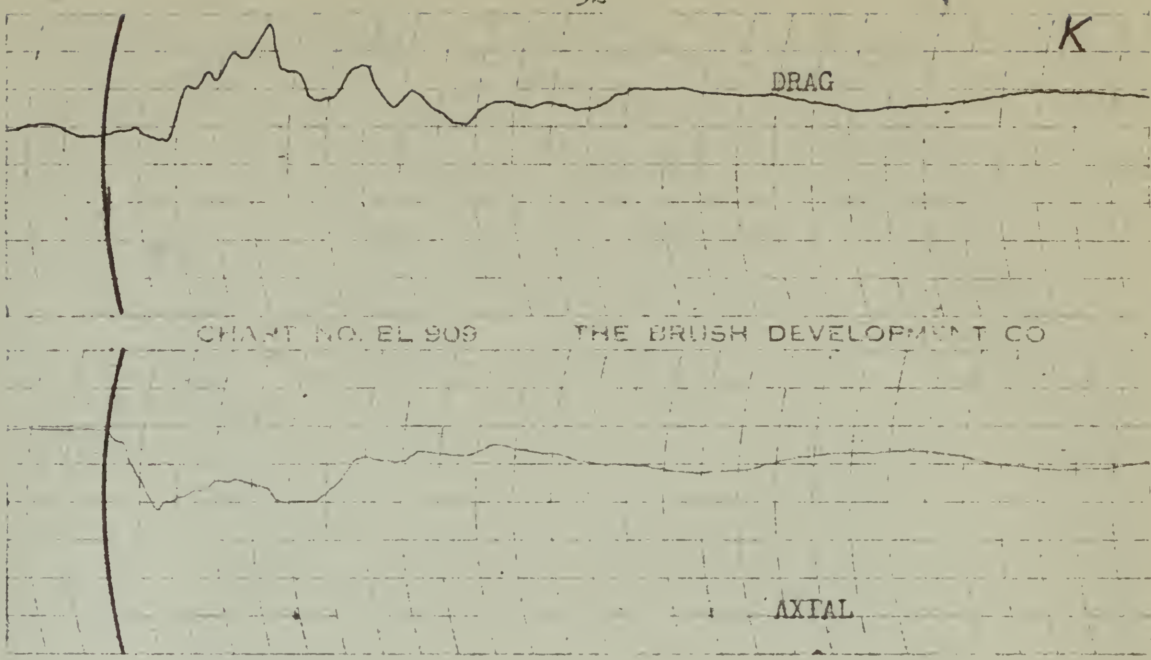

CALIBRATION:
DRAG - 1 mm. = 220#
AXIAL - 5 mm. = 930#
CANTILEVER - 1 mm. = .375 in.
POTENTIOMETER - REFER CURVE "B" FIG. 6

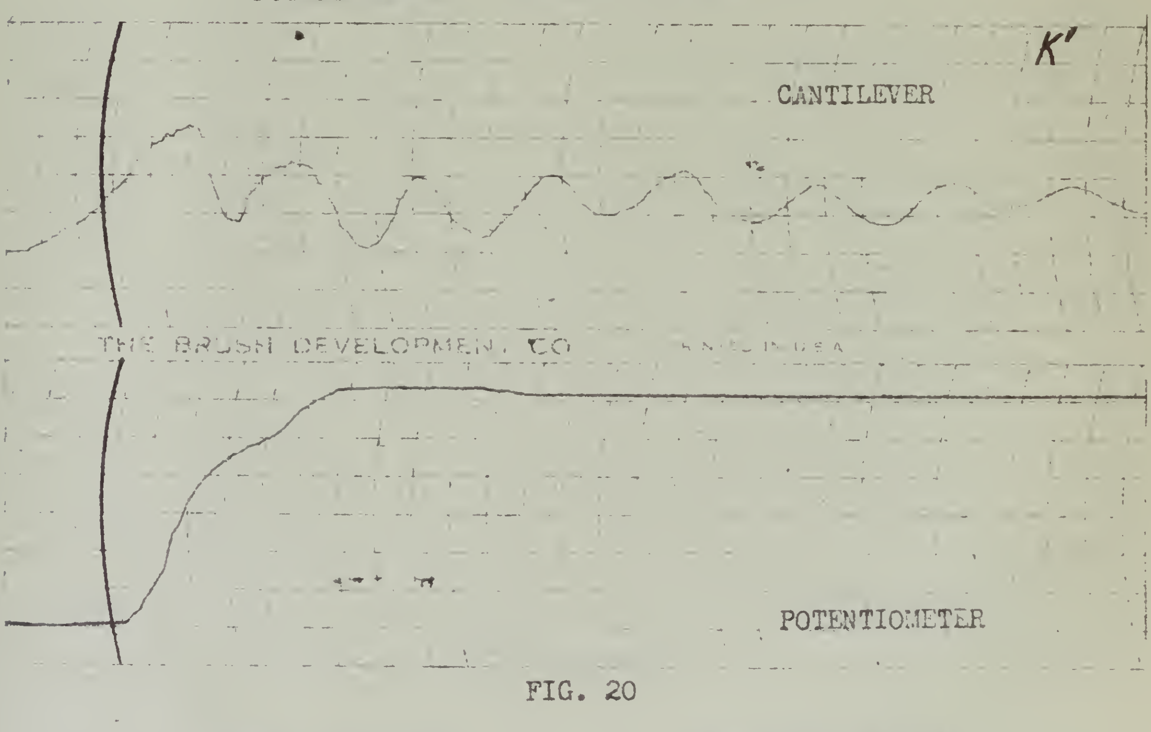

FIG. 20

DATE: 7/10/49
STRUT ANGLE 26°
WEIGHT 1060#

TIRE PRESSURE 24#
LANDING VELOCITY 60 F.P.S.
DROPPING VELOCITY 4 F.P.S.
PAPER SPEED 125 mm./sec.

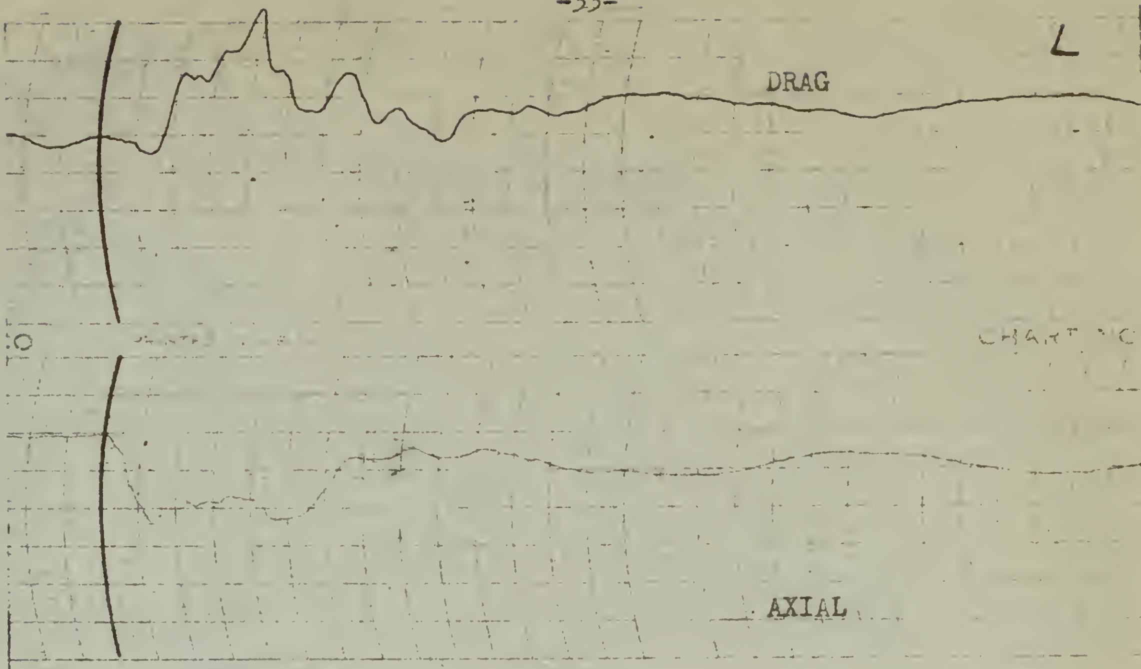

CALIBRATION:

DRAG - 1 mm. = 220#
AXIAL - 5 mm. = 930#
CANTILEVER - 1 mm. = .375 in.
POTENTIOMETER - REFER CURVE "B" FIG. 6

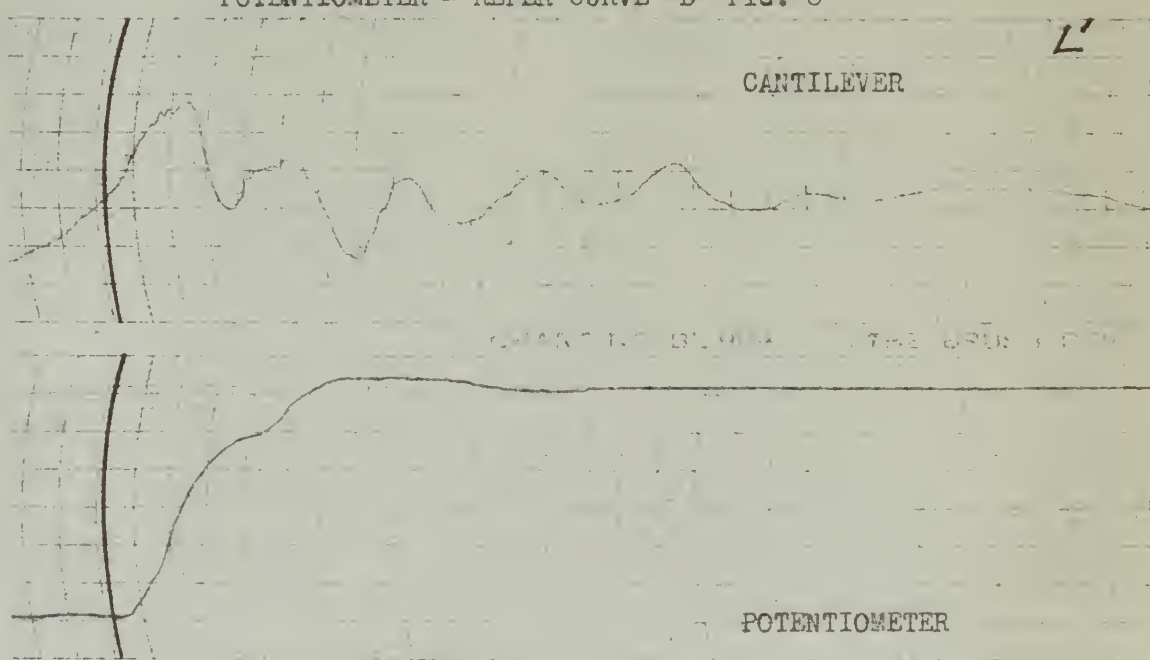

FIG. 21

DATE: 7/10/49
STRUT ANGLE 26°
WEIGHT 1060#

TIRE PRESSURE 24#
LANDING VELOCITY 60 F.P.S.
DROPPING VELOCITY 5 F.P.S.
PAPER SPEED 125 mm./sec.

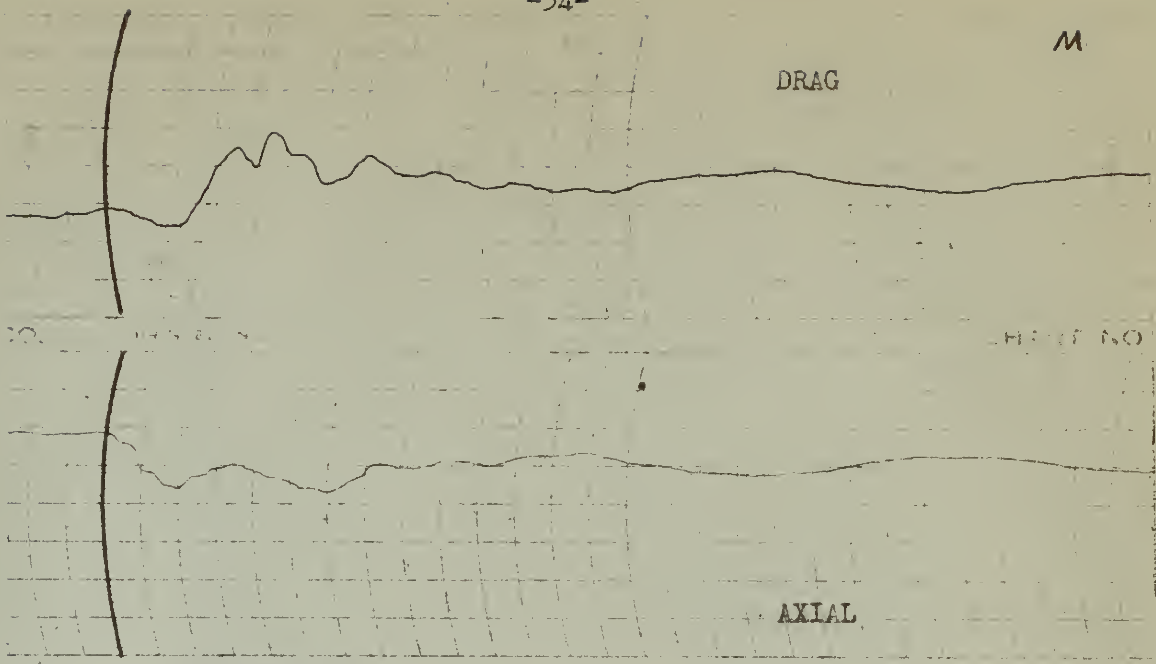

CALIBRATION:
DRAG - 1 mm. = 220#
AXIAL - 5 mm. = 930#
CANTILEVER - 1 mm. = .375 in.
POTENTIOMETER - REFER CURVE "B" FIG. 6

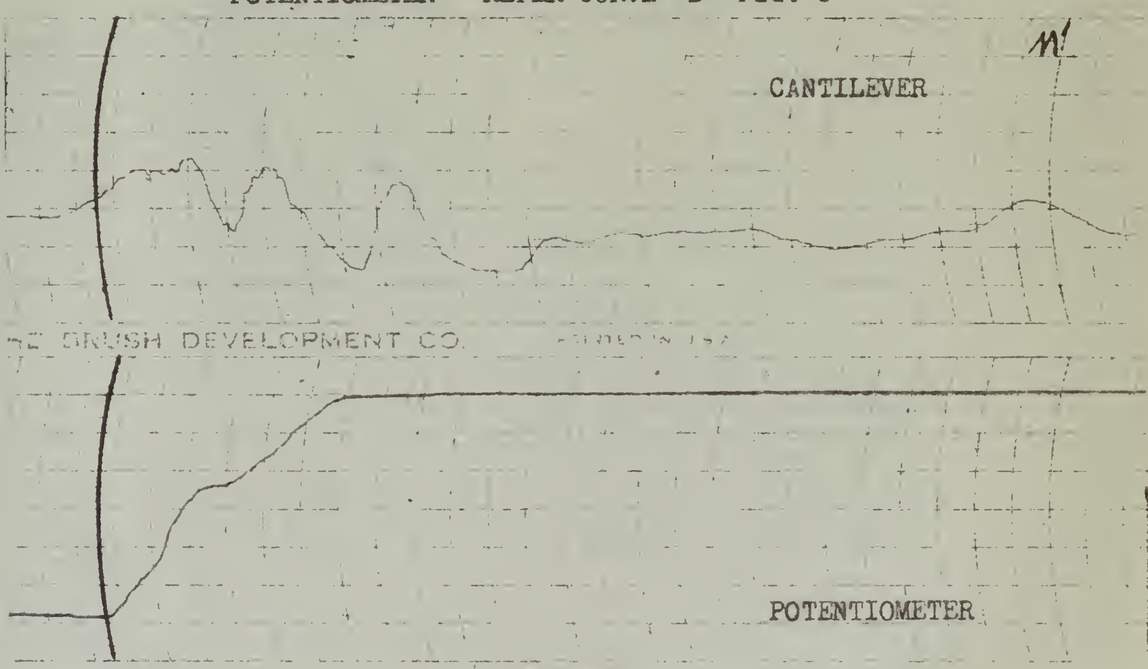

FIG. 22

DATE: 7/10/49
STRUT ANGLE 28°
WEIGHT 1060#

TIRE PRESSURE 24#
LANDING VELOCITY 59.2 F.P.S.
DROPPING VELOCITY 2 F.P.S.
PAPER SPEED 125 mm./sec.

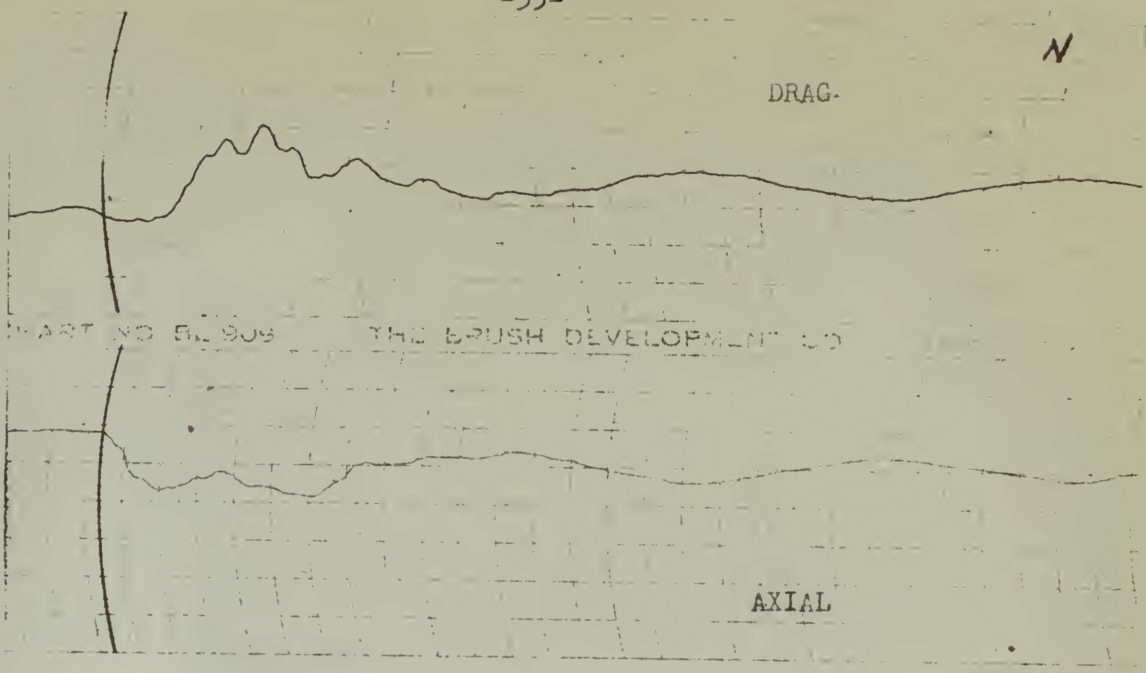

CALIBRATION:

DRAG	- 1 mm. = 220#
AXIAL	- 5 mm. = 930#
CANTILEVER	- 1 mm. = .375 in.
POTENTIOMETER	- REFER CURVE "B" FIG. 6

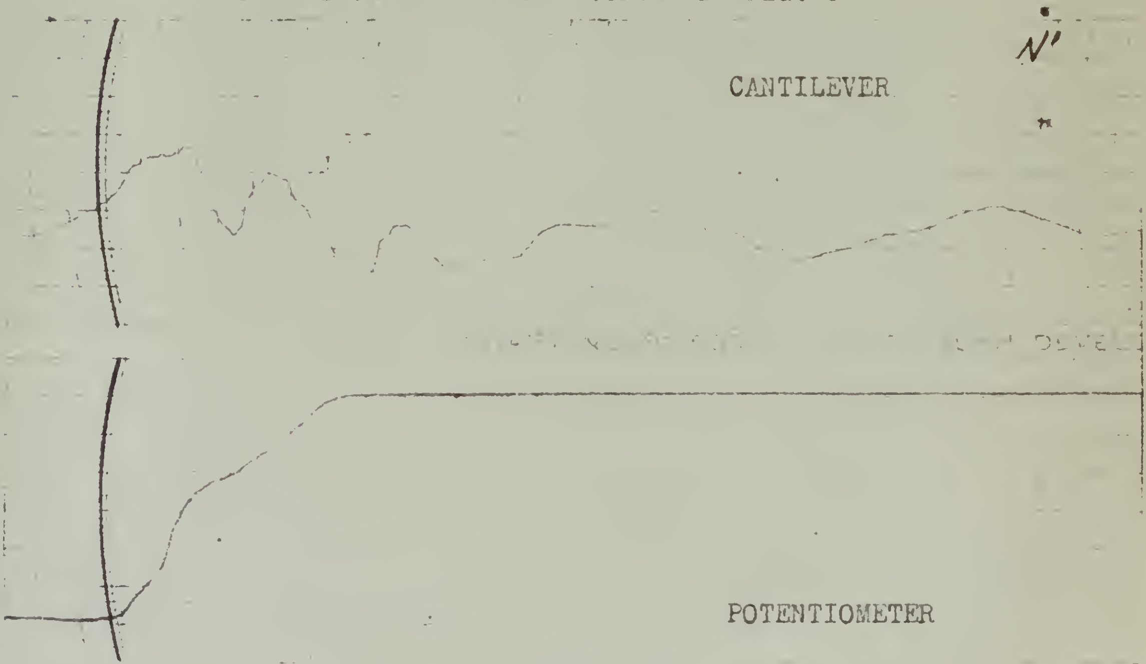

FIG. 23

DATE: 7/10/49
STRUT ANGLE 28°
WEIGHT 1060#

TIRE PRESSURE 24#
LANDING VELOCITY 59.2 F.P.S.
DROPPING VELOCITY 3 F.P.S.
PAPER SPEED 125 mm./sec.

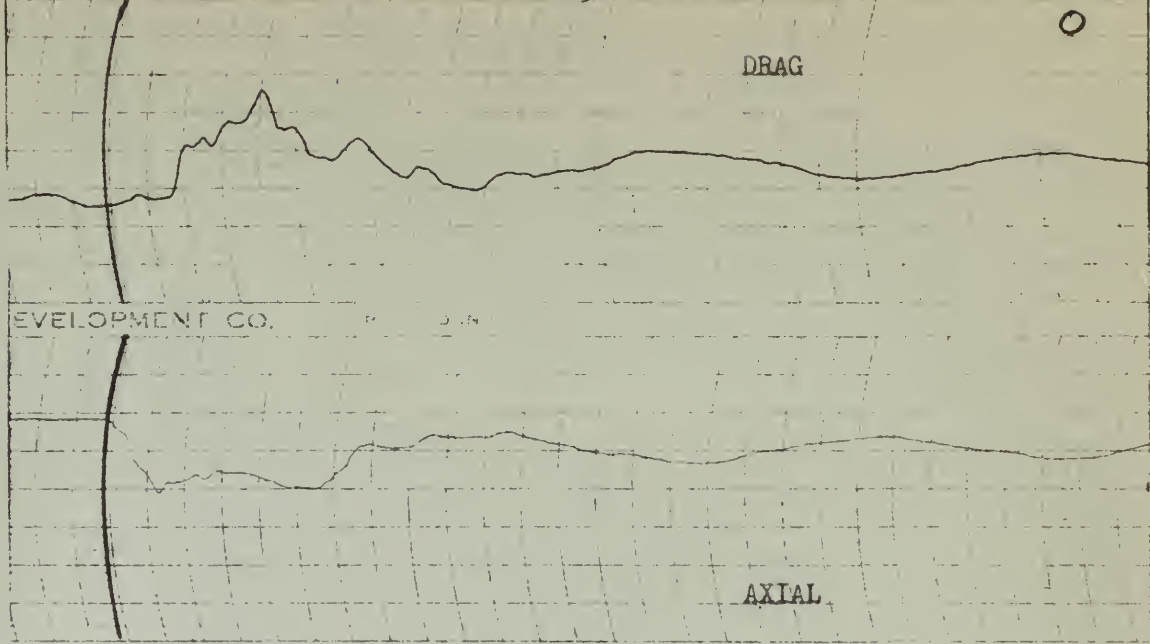

CALIBRATION:

DRAG	- 1 mm. = 220#
AXIAL	- 5 mm. = 930#
CANTILEVER	- 1 mm. = .375 in.
POTENTIOMETER	- REFER CURVE "B" FIG. 6

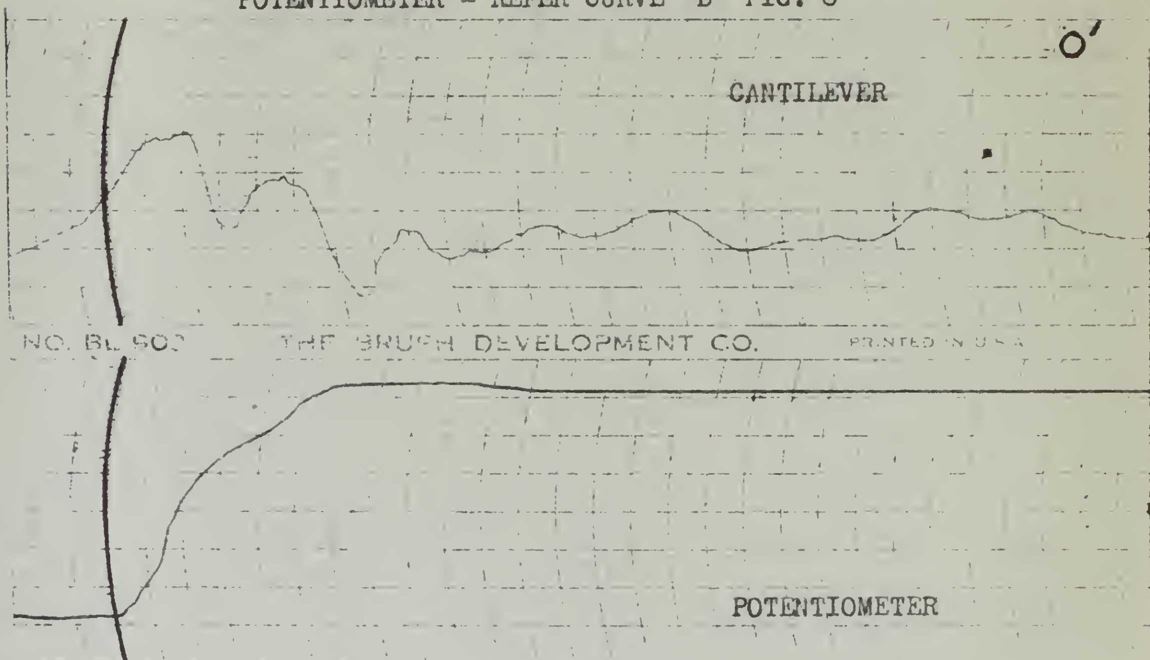

FIG. 24

DATE: 7/10/49
STRUT ANGLE 28°
WEIGHT 1060#

TIRE PRESSURE 24#
LANDING VELOCITY 59.2 F.P.S.
DROPPING VELOCITY 4 F.P.S.
PAPER SPEED 125 mm./sec.

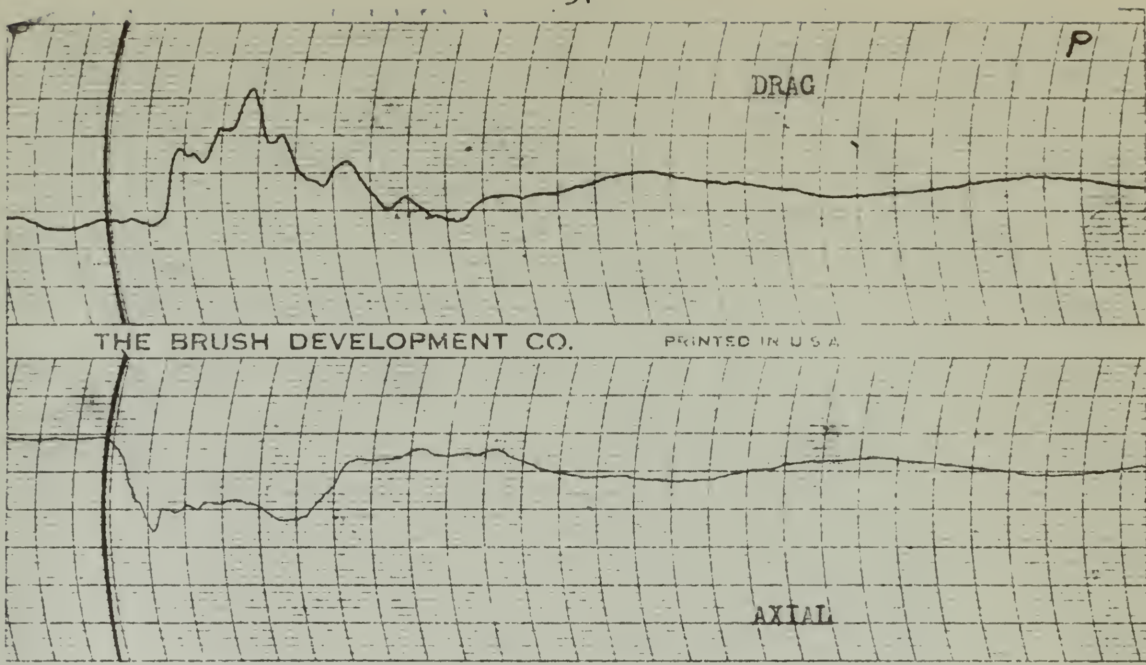

CALIBRATION:
DRAG - 1 mm. = 220#
AXIAL - 5 mm. = 930#
CANTILEVER - 1 mm. = .375 in.
POTENTIOMETER - REFER CURVE "B" FIG. 6

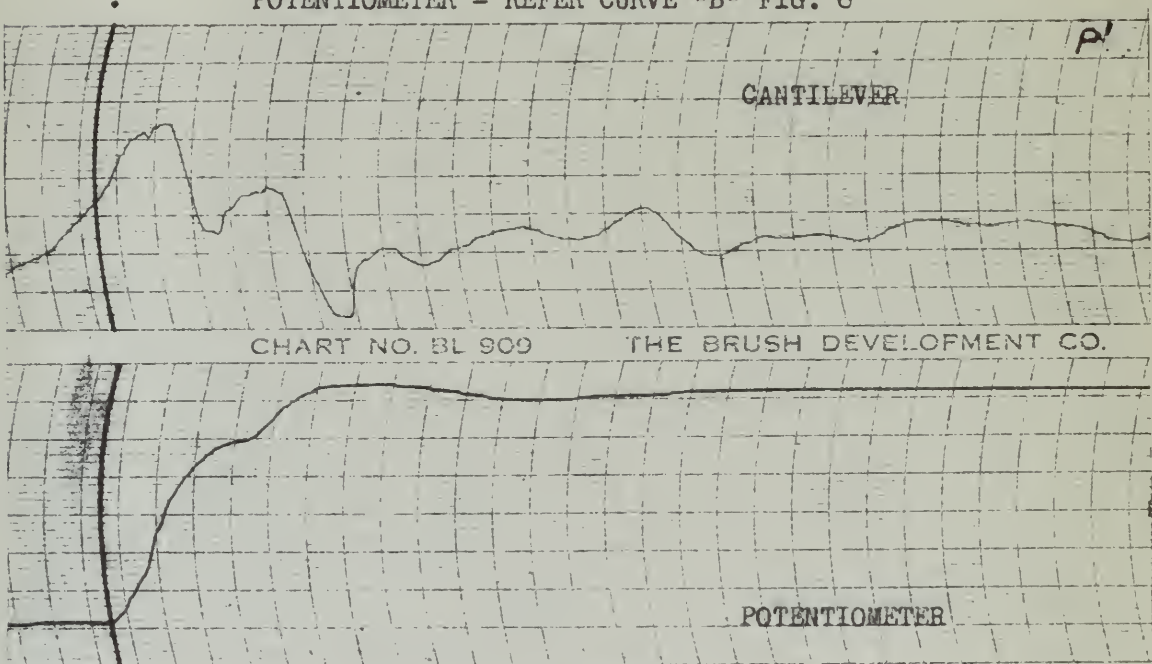

FIG. 25

DATE: 7/10/49
STRUT ANGLE 28°
WEIGHT 1060#

TIRE PRESSURE 24#
LANDING VELOCITY 59.2 F.P.S.
DROPPING VELOCITY 5 F.P.S.
PAPER SPEED 125 mm./sec.

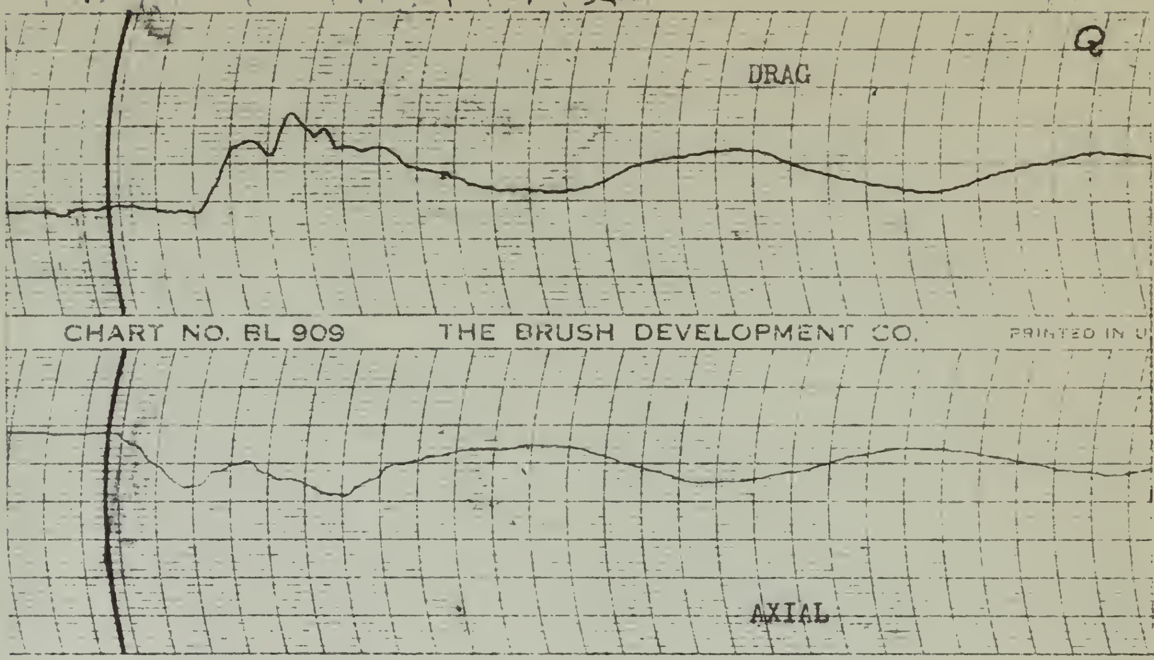

CALIBRATION:

DRAG	- 1 mm. = 220#	
AXIAL	- 5 mm. = 930#	
CANTILEVER	- 1 mm. = .375 in.	
POTENTIOMETER	- REFER CURVE "B" FIG. 6	

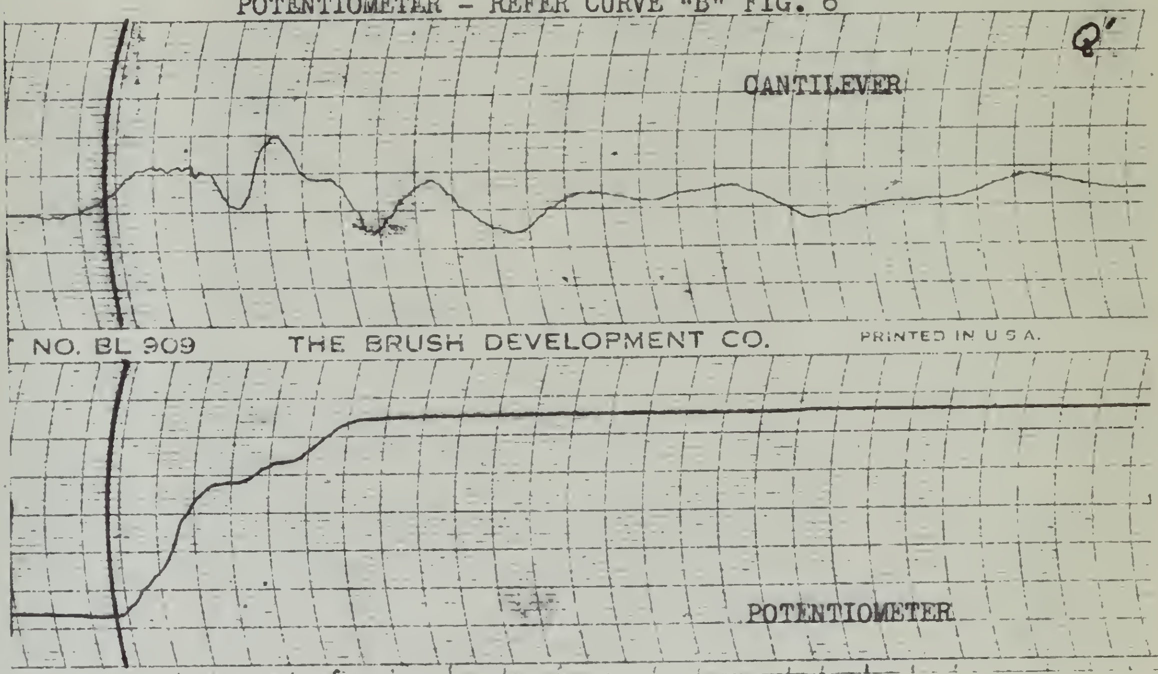

FIG. 26

DATE: 7/10/49
STRUT ANGLE 30°
WEIGHT 1060#

TIRE PRESSURE 24#
LANDING VELOCITY 57.5 F.P.S.
DROPPING VELOCITY 2 F.P.S.
PAPER SPEED 125 mm./sec.

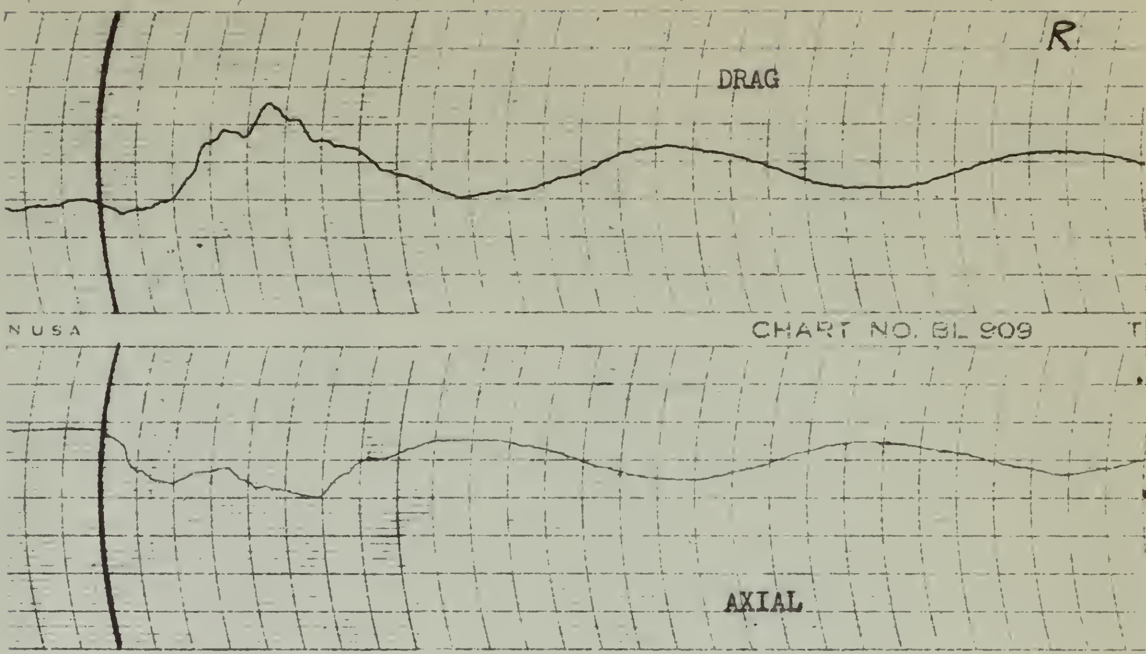

CALIBRATION:

DRAG	- 1 mm. = 220#
AXIAL	- 5 mm. = 930#
CANTILEVER	- 1 mm. = .375 in.
POTENTIOMETER	- REFER CURVE "B" FIG. 6

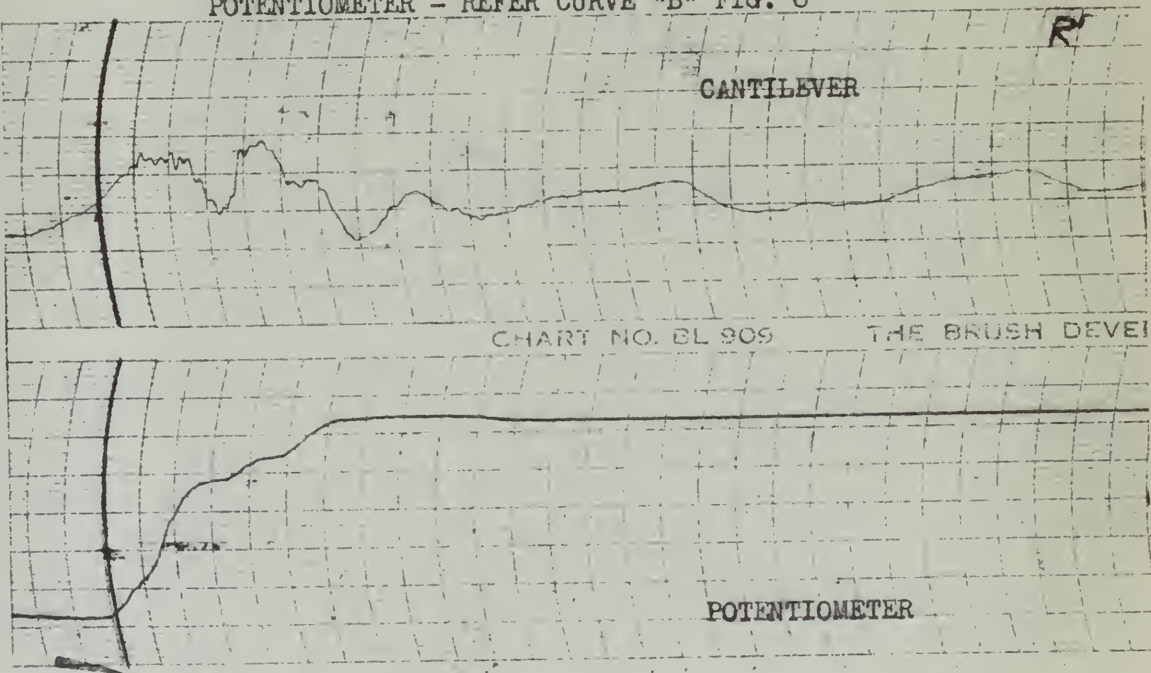

FIG. 27

DATE: 7/10/49
STRUT ANGLE 30°
WEIGHT 1060#

TIRE PRESSURE 24#
LANDING VELOCITY 57.5 F.P.S.
DROPPING VELOCITY 3 F.P.S.
PAPER SPEED 125 mm./sec.

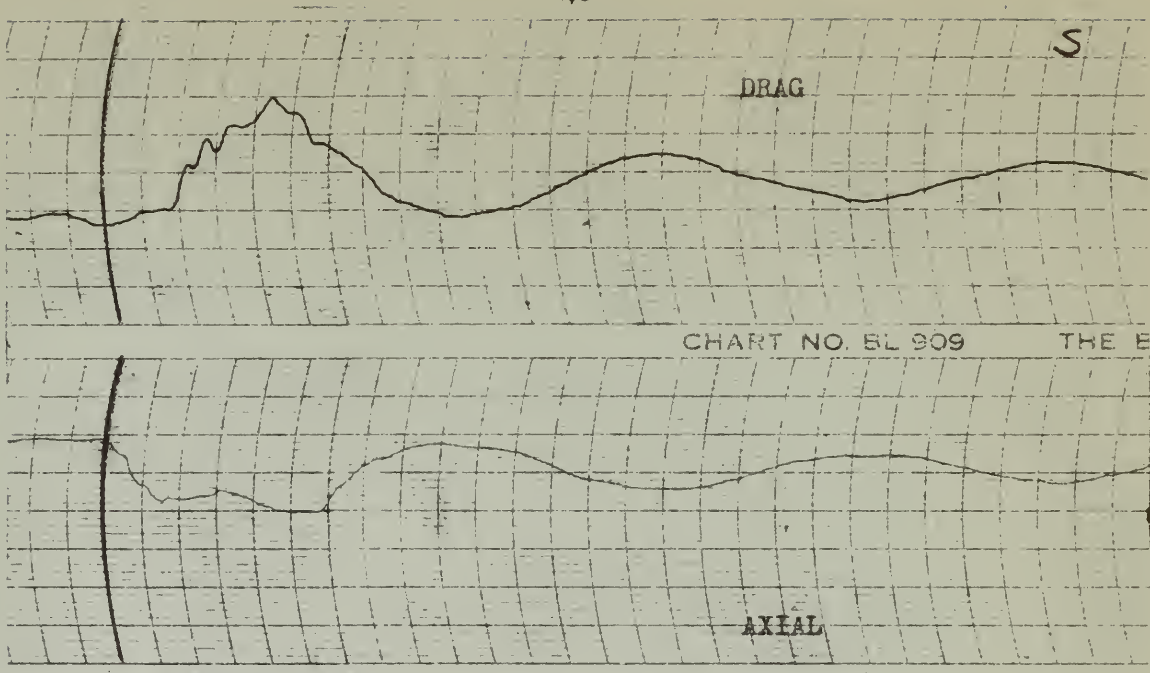

CALIBRATION:

DRAG	- 1 mm. = 220#
AXIAL	- 5 mm. = 930#
CANTILEVER	- 1 mm. = .375 in.
POTENTIOMETER	- REFER CURVE "B" FIG. 6

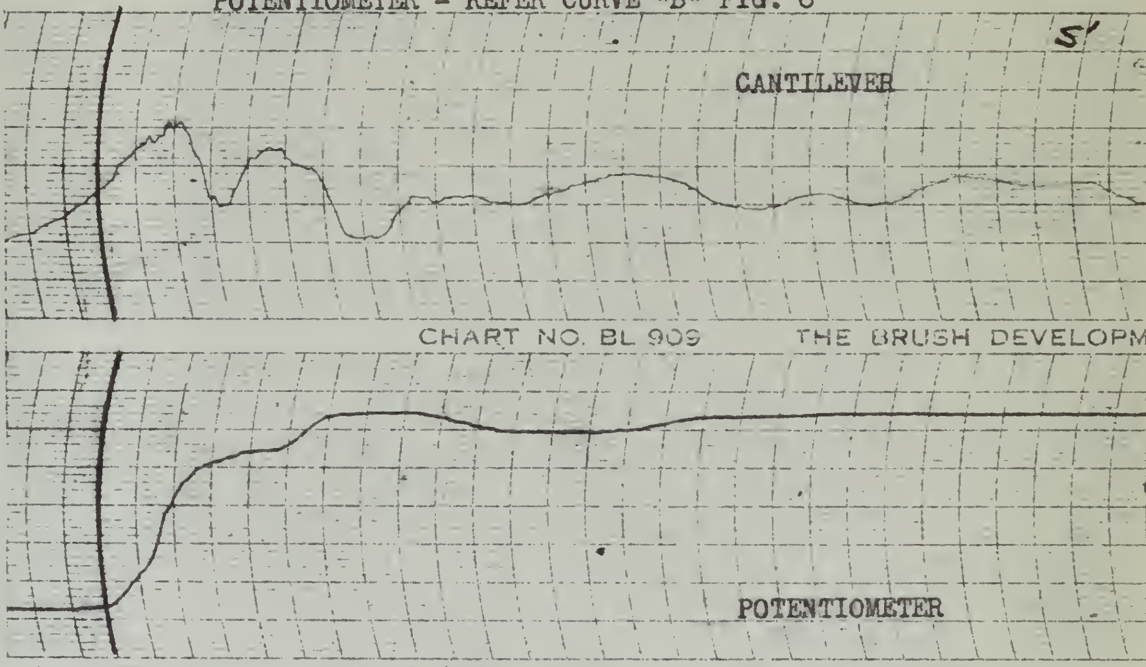

FIG. 28

DATE: 7/10/49
STRUT ANGLE 30°
WEIGHT 1060#

TIRE PRESSURE 24#
LANDING VELOCITY 57.5 F.P.S.
DROPPING VELOCITY 4 F.P.S.
PAPER SPEED 125 mm./sec.

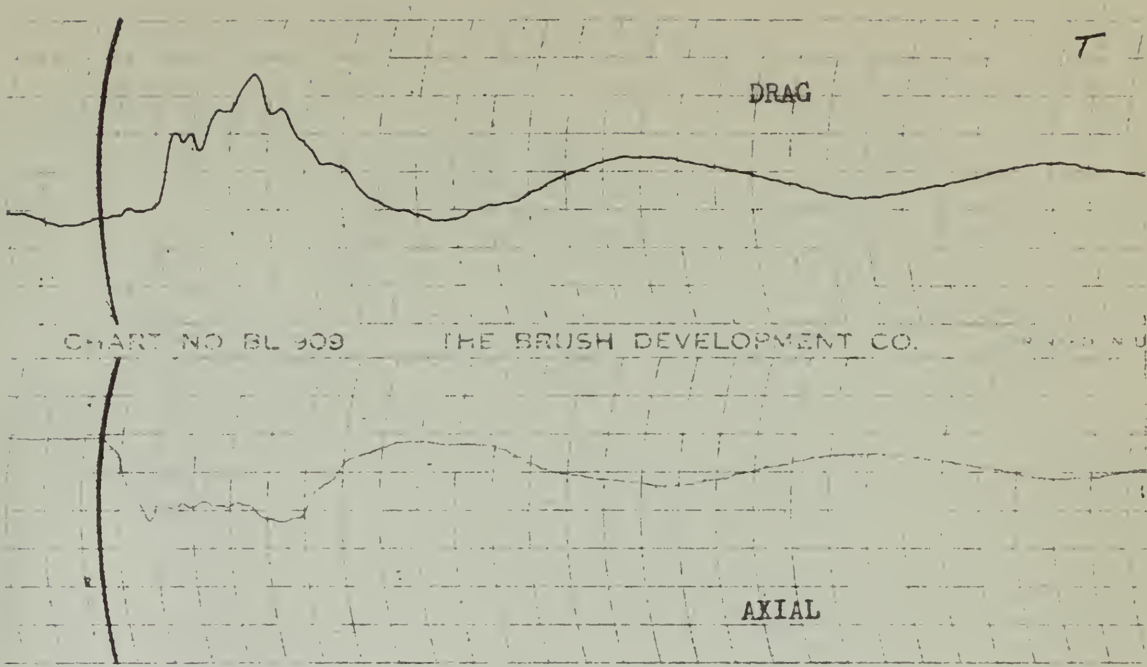

CALIBRATION:

DRAG - 1 mm. = 220#

AXIAL - 5 mm. = 930#

CANTILEVER - 1 mm. = .375 in.

POTENTIOMETER - REFER CURVE "B" FIG. 6

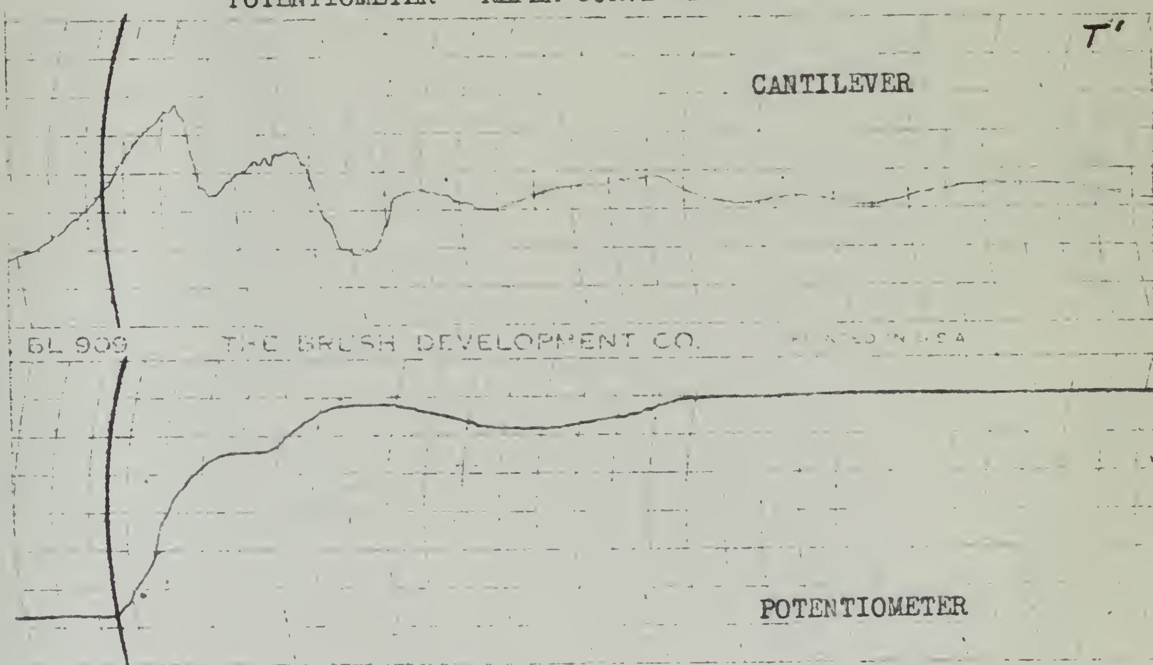

FIG. 29

DATE: 7/10/49
STRUT ANGLE 30°
WEIGHT 1060#

TIRE PRESSURE 24#
LANDING VELOCITY 57.5 F.P.S.
DROPPING VELOCITY 5 F.P.S.
PAPER SPEED 125 mm./sec.

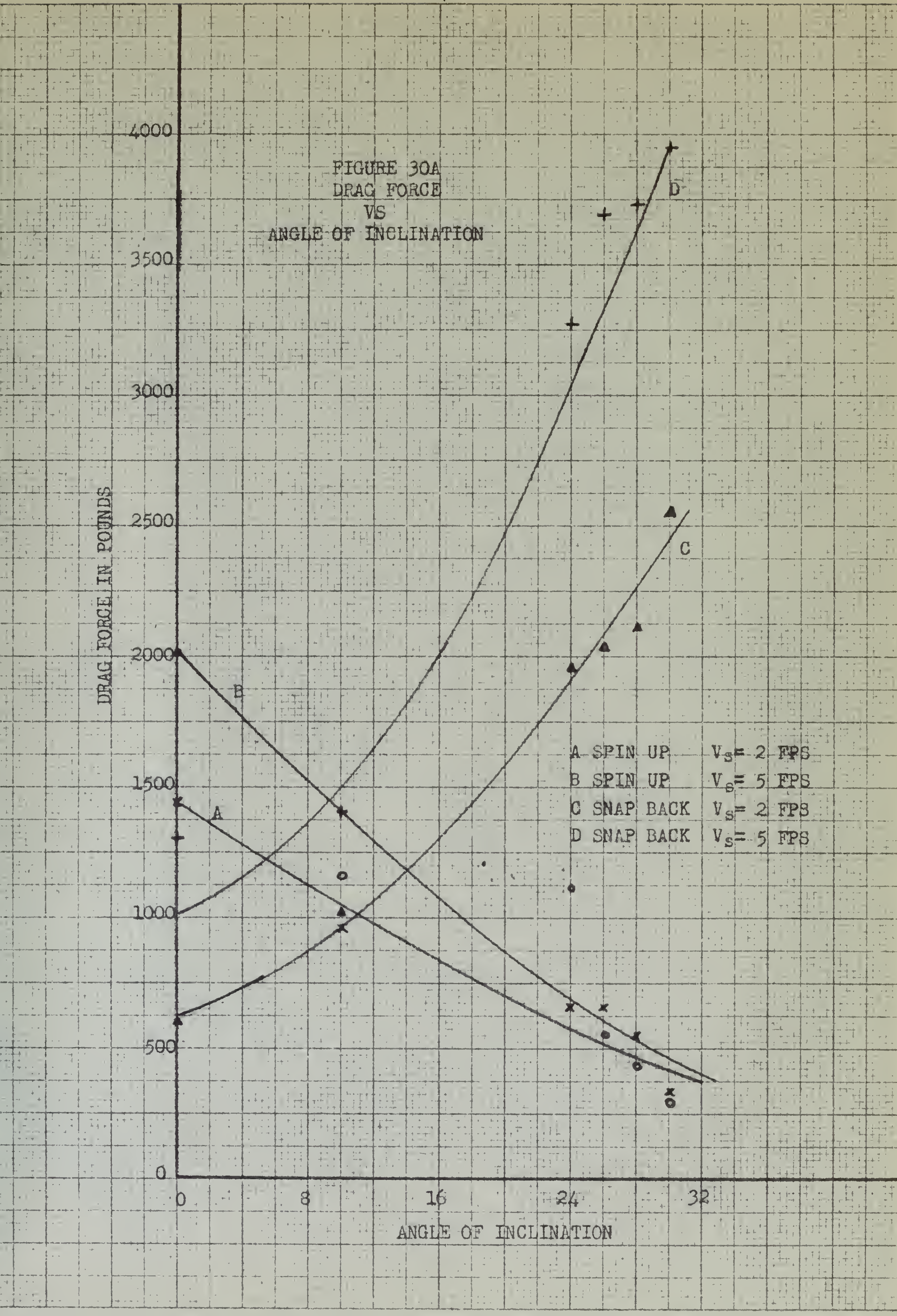
FIGURE 30A
DRAG FORCE
VS
ANGLE OF INCLINATION
DRAG FORCE IN POUNDS
4000
3500
3000
2500
2000
1500
1000
500
0
0
8
16
24
32
ANGLE OF INCLINATION
A
B
C
D
A SPIN UP V_S= 2 FPS
B SPIN UP V_S= 5 FPS
C SNAP BACK V_S= 2 FPS
D SNAP BACK V_S= 5 FPS

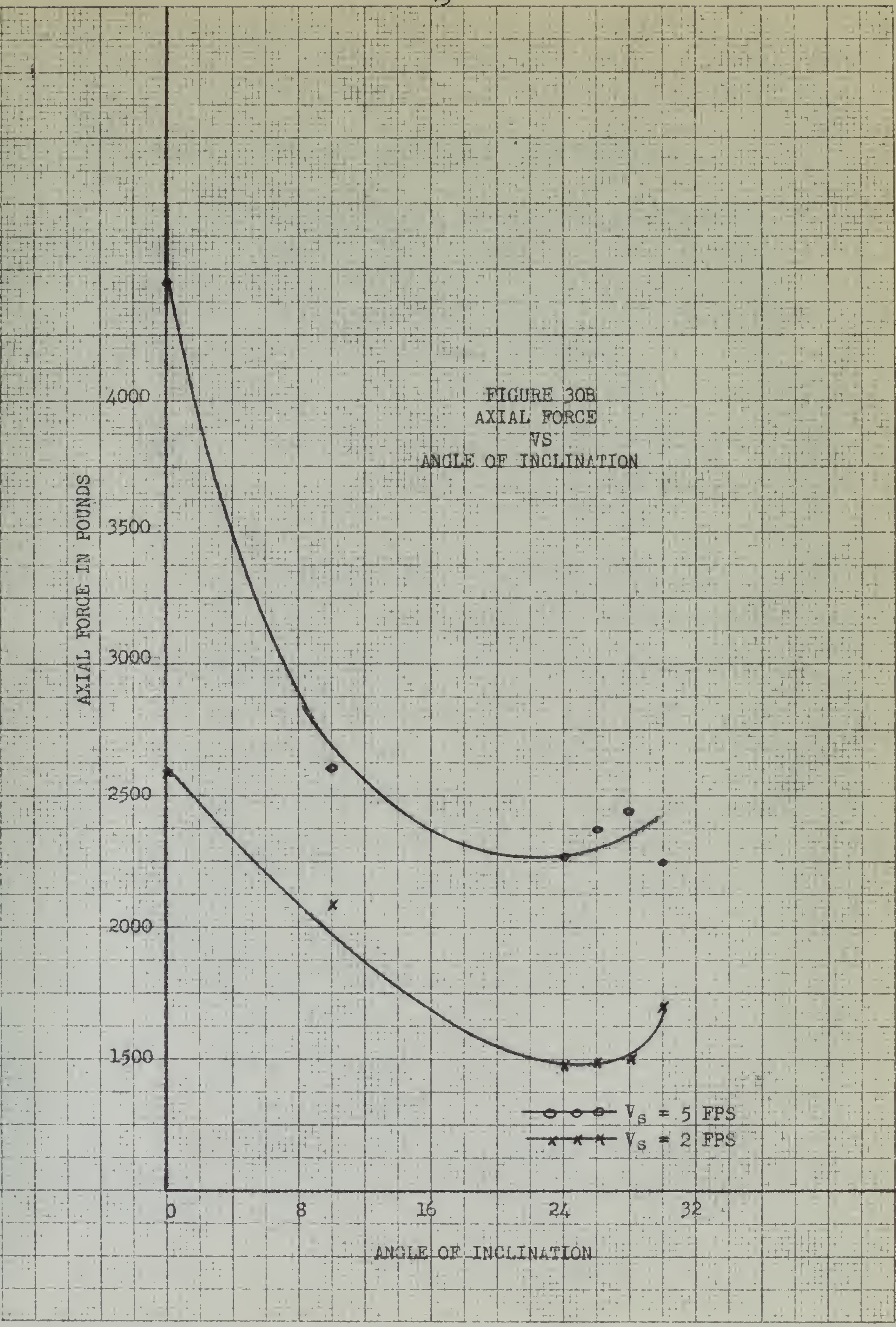
FIGURE 30B
AXIAL FORCE
VS
ANGLE OF INCLINATION
AXIAL FORCE IN POUNDS
4000
3500
3000
2500
2000
1500
0
8
16
24
32
ANGLE OF INCLINATION
V_s = 5 FPS
V_s = 2 FPS

COMPARISON OF TEST AND THEORY

An analytical study of the dynamic forces in landing gear of aircraft is developed in the Appendix. A comparison will be made between the results obtained by test and the results obtained by the analytical approach.

In the example problem developed in the Appendix for an angle of twenty-four degrees and a sinking velocity of three feet per second the displacement equation for wheel, or m_2 is:

$$z_2 = .001137e^{-3.01t} + .001086e^{-158.679t}$$
$$+ e^{-8.155t}(.1368 \sin 15.235t - .1136 \cos 15.235t)$$

The following displacements are obtained:

at $t = .02$ second

$z_2 = .4472$ inch

at $t = .07$ second

$z_2 = 2.41$ inches

From test data of Figure 16, the following displacements are obtained:

at $t = .02$ second

$z_2 = .75$ inch

at $t = .07$ second

$z_2 = 2.25$ inches

The above values have been evaluated as true tire deflection. The test data shows greater tire deflections

shortly after impact than is obtained by analytical methods, while after a longer period of time the analytical method gives greater tire deflection than is indicated by the test data. This indicates that the spring characteristic of the tire is not a constant as used in the analytical method, but varies with displacement.

The theoretical equation for the displacement of m_1 is:

$$z_1 = -.3534e^{-3.01t} - .0001583e^{-158.879t}$$
$$+ e^{-8.155t}(.04206 \sin 16.235t - .1584 \cos 16.235t)$$

The following displacements are obtained:

at $t = .02$ second

$z_1 = .762$ inch

at $t = .07$ second

$z_1 = 3.41$ inches

For the same time periods the test data produces the displacements below:

at $t = .02$ second

$z_1 = 1.05$ inches

at $t = .07$ second

$z_1 = 3.95$ inches

The test data shows greater displacements for m_1 than are calculated analytically. This indicates that the spring constant used in the analytical calculation is very small on initial compression and that the damping is somewhat less than calculated. More exact spring and

damping constants would improve the correlation between test and analytical results.

The maximum drag force and time of maximum drag force for angle of 0 degree are calculated in an example problem in the Appendix. The following results are obtained:

t_s = .081 second

$P_{x\ max}$ = 2140 pounds

Test data from Figure 7 produce the following results:

t_s = .08 second

P_x max = 1550 pounds

The time at which the maximum drag force occurs is the same for analytical and test results. The calculated maximum drag force is much larger than the maximum drag force obtained from test results. This large variation between theoretical and test results may be due to the fact that the coefficient of friction was assumed to be constant and $P_{\frac{zt}{t}}$ was assumed a constant. The assumption that the coefficient of friction is a constant is erroneous and further investigation should be conducted to determine its value.

The optimum angle of suspension, as calculated in the Appendix, is 23° 31', whereas test results indicate the optimum angle of suspension to be approximately ten degrees. This necessitates a revision in the analytical method of calculating the optimum angle of suspension. The analytical

results were also computed from test data, which requires further verification. The preceding improvement in analytical evaluation accompanied with more test data to definitely establish the optimum angle will no doubt produce better agreement between theoretical and test results.

results were also computed from each data, which provides further modifications. The preceding improvement in analytical evaluation accompanied with more test data to [illegible] establish the optimum angle will be [illegible] better agreement between theoretical and test results.

CONCLUSIONS

1. To produce equal bending moments during spin up and snap back of the strut, the optimum angle for suspending an SNJ type aircraft strut is approximately ten degrees.

2. Minimum axial forces are produced by suspending the strut at an angle of approximately twenty-four degrees.

3. Frictional forces impair the operation of the oleo and warrant further investigation.

4. The coefficient of friction of aircraft tires during landing impact should be investigated more thoroughly.

5. The load deflection characteristics of a rotating aircraft tire should be investigated more thoroughly.

APPENDIX

THEORY OF DYNAMIC FORCES IN LANDING GEAR OF AIRCRAFT

A. The Spring Mass System for Landing Gear

For the investigation of the properties of a landing as shown in Figure 31A, it may be considered as a simplified system of two masses and two spring systems as shown in Figure 31B. Mass m_1 represents half of the mass above the landing gear, including the airplane and those parts of the shock strut rigidly attached to it. Mass m_2 includes the wheel with tire and the parts of the gear attached to them; m_2 is small compared to m_1. The shock strut or oleo will have both damping and spring characteristics. The tire will also exhibit a spring characteristic.

This system drops to the ground with a sinking velocity of V_s. Neglecting lateral forces and bending moments acting on the strut, the vertical forces and motions can be found analytically. Considering no lift acting on the airplane these differential equations of motion are:

$$m_1 \ddot{z}_1 + k_1(z_1 - z_2) + c_1(\dot{z}_1 - \dot{z}_2) = 0$$

$$m_2 \ddot{z}_2 + k_2 z_2 - k_1(z_1 - z_2) - c_1(\dot{z}_1 - \dot{z}_2) = 0$$

By letting

$$z_1 = Ae^{st}$$

$$z_2 = Be^{st}$$

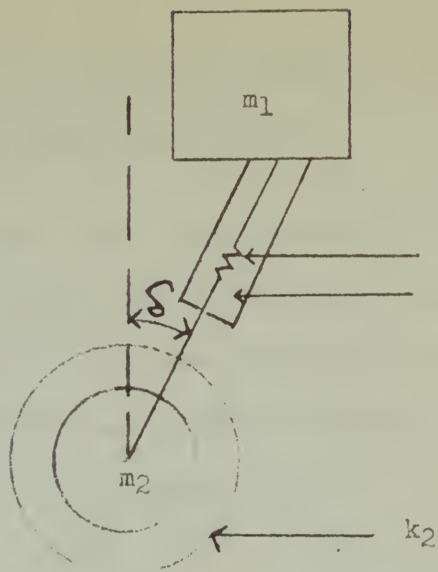

FIGURE 31A
LANDING GEAR SYSTEM

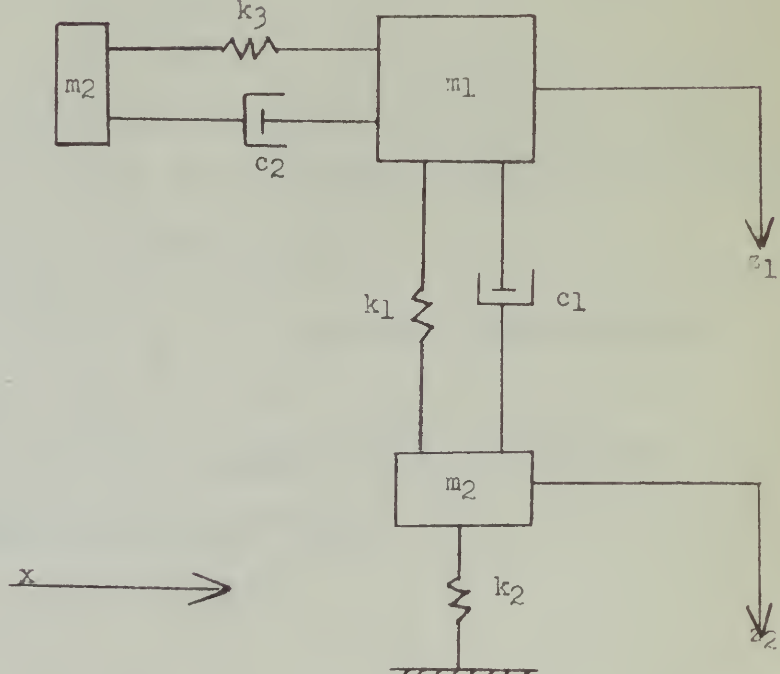

FIGURE 31B
SPRING MASS SYSTEM

the following equation is formed:

$$s^4 + as^3 + bs^2 + cs + d = 0$$

The solution of this equation results in four roots. These roots may be either real or complex. If all roots are real, critical damping has been reached and subsidence motion occurs. Complex roots indicate damped vibratory motion. The equations of motion become:

$$z_1 = Ae^{s_1t} + Be^{s_2t} + Ce^{s_3t} + De^{s_4t}$$

$$z_2 = A^1e^{s_1t} + B^1e^{s_2t} + C^1e^{s_3t} + D^1e^{s_4t}$$

where $A^1 = \eta_1 A$

$B^1 = \eta_2 B$

$C^1 = \eta_3 C$

$D^1 = \eta_4 D$

By imposing four boundary conditions on the above equations of motion, the four unknown constants may be found.

At time of impact or $t = 0$

$$\left.\begin{aligned} z_1 &= -\Delta_1 \\ z_2 &= -\Delta_2 \end{aligned}\right\} \quad \text{which are static deflections}$$

$\dot{z}_1 - \dot{z}_2 = V_{s_0}$ (Sinking velocity of airplane)

Thus the equations become:

$$-\Delta_1 = A + B + C + D$$

$$-\Delta_2 = \eta_1 A + \eta_2 B + \eta_3 C + \eta_4 D$$

$$V_{s_0} = As_1 + Bs_2 + Cs_3 + Ds_4$$

$$V_{s_0} = \eta_1 As_1 + \eta_2 Bs_2 + \eta_3 Cs_3 + \eta_4 Ds_4$$

The vertical force due to the vertical motion then becomes:

$$F_{zt} = k_2(z_2 + \Delta_2)$$

$$F_{zt} = k_2\Delta_2 + k_2(\eta_1 Ae^{s_1 t} + \eta_2 Be^{s_2 t} + \eta_3 Ce^{s_3 t} + \eta_4 De^{s_4 t})$$

As an example problem, consider the case of the strut under test at an angle of 24° and a sinking velocity of 3 feet per second.

$$m_1 = 29.16 \frac{\text{lb.-sec.}^2}{\text{ft.}}$$

$$m_2 = 3.76 \frac{\text{lb.-sec.}^2}{\text{ft.}}$$

The damping constant is found by making use of the test data. The slope of the potentiometer curve at time t is used to find the relative velocity between m_1 and m_2. This is the velocity at which an integrated part of the strut is moving through a viscous medium. The motion through the viscous medium produces damping. The axial force in the strut at time t less the spring force due to compression of the oleo is the force due to damping. Then the damping constant

$$c = \frac{F}{\frac{ds}{dt}} = 653 \frac{\text{lb.-sec.}}{\text{ft.}}$$

k_2 = 11.250 lb/ft (Reference Figure 5A)

k = 1,685 lb/ft (Reference Figure 5B)

$\delta = 24^{\circ}$

$c_1 = c \cos 24^{\circ}$

$= 595 \ \frac{\text{lb.sec.}}{\text{ft.}}$

$k_1 = k \cos 24^{\circ}$

$=$ 1,535 lb/ft

k_2 = 11,250 lb/ft

The static deflections from equilibrium position at $t = 0$ are:

$z_1 = \Delta_1 = -.512$ ft.

$z_2 = \Delta_2 = -.094$ ft.

$\dot{z}_1 = V_{s_0} = 3$ ft/sec.

$\dot{z}_2 = V_{s_0} = 3$ ft/sec.

The equations of motion are:

$$29.16\,\ddot{z}_1 + 1535(z_1 - z_2) + 595(\dot{z}_1 - \dot{z}_2) = 0$$

$$3.76\,\ddot{z}_2 + 11{,}250 z_2 - 1535(z_1 - z_2) - 595(\dot{z}_1 - \dot{z}_2) = 0$$

By letting

$z_1 = Ae^{st}$

$z_2 = Be^{st}$

the following equation is formed:

$$s^4 + 178s^3 + 3445s^2 + 61{,}000s + 157{,}900 = 0$$

The roots of this equation are:

$s_1 = -3.01$

$s_2 = -158.679$

$s_3 = -8.155 + 16.235i$

$s_4 = -8.155 - 16.235i$

The equation of motion becomes

$$z_1 = Ae^{-3.01t} + Be^{-158.679t} + e^{-8.155t}(Ce^{16.235it} + De^{-16.235it})$$

$$z_2 = A^1e^{-3.01t} + B^1e^{-158.679t} + e^{-8.155t}(C^1e^{16.235it} + D^1e^{-16.235it})$$

$A = .3534$

$B = -.0001583$

$C = -.07922 - .02103i$

$D = -.07922 + .02103i$

$A^1 = .0011379$

$B^1 = .001086$

$C^1 = -.05182 - .06840i$

$D^1 = -.05182 + .06840i$

$$z_1 = -.3534e^{-3.01t} - .0001583e^{-158.679t} + e^{-8.155t}(.04206 \sin 16.235t - .1584 \cos 16.235t)$$

$$z_2 = .001137e^{-3.01t} + .001086e^{-158.679t} + e^{-8.155t}(.1368 \sin 16.235t - .1136 \cos 16.235t)$$

B. The Drag Forces for the Spin-Up of the Wheels

As an aircraft wheel touches the ground, a horizontal drag force appears. This drag force accelerates the wheel rotation up to landing speed. The ratio between the horizontal drag force and the vertical tire load is expressed by $\mu = \frac{P_x}{P_{zt}}$. There are several kinds of contact between the tire and landing surface during the acceleration of the wheel. This contact varies from complete sliding at time of impact to pure adhesion at the time the wheel has accelerated to the landing velocity. In this analysis μ will be treated as a constant.

Assuming a constant radius r_t for the wheel since the change in radius is small during the acceleration period, the acceleration equation becomes

$$P_x r_t = I_w \omega \frac{d^2\theta}{dt^2}$$

or

$$\mu P_{zt} r_t = I_w \ddot{\theta}$$

During the period of acceleration P_{zt} is assumed to be a linear function such that

$$P_{zt} = Kt$$

where K is a constant

$$\mu K t \, r_t = I_w \ddot{\theta}$$

Integrating with respect to t

$$\dot{\theta} = \mu \frac{K t^2 r_t}{2 I_w} + K$$

at $t = 0$, $\dot{\theta} = 0$

therefore $K = 0$

at $t = t_s$, $\dot{\theta} = \dfrac{V_L}{r_t}$

t_s = time of slip of tire on ground

$$\frac{V_L}{r_t} = \frac{\mu R\, t_s^{\,2}\, r_t}{2I_w}$$

$$t_s = \sqrt{\frac{2I_W\, V_L}{\mu R r_t^{\,2}}}$$

The maximum drag force occurs at $t = t_s$ thus,

$$F_{xmax} = \mu R t_s$$

As an example problem consider the case of the strut suspended at an angle of 0^o.

Since the coefficient of friction is not known it is taken as the ratio of the drag force in Figure 7 over force due to tire deflection in Figure 7 at a given time t.

$t =$ .04 sec.

$\mu =$ .63

$R = \dfrac{F_{zt}}{t}$

This value of R is not known and is taken as the ratio of the force due to tire deflection over time from Figure 7.

$t = .04$

$R = 42{,}000$ lb/sec.

I_w = 2.1 slugs-ft^2 (Reference Report TSEAL-23-4263-46-4, Engineering Laboratory Air Material Command)

V_L = 52.5 ft/sec.

r_t = 1.12 ft.

$$t_s = \sqrt{\frac{2 \times 2.1 \times 52.5}{.63 \times 42{,}000 \times (1.12)^2}}$$

$= .081$ second

The maximum drag force occurs when slipping stops.

$$F_{x\ max} = \mu t_s N$$

$= .63 \times .81 \times 42{,}000$

$= 2140$ lb.

C. Optimum Angle of Suspension

In order to calculate the optimum angle of suspension it is necessary to take into consideration the snap back of the strut after the initial impact has taken place. This snap back force is due to the inertia force of the wheel mass acting upon the strut, which acts as a cantilever spring. The differential equation of motion during impact is

$$m_2\ddot{x} + cx = P_x$$

$$P_x = \mu Rt$$

$$m_2\ddot{x} + cx = \mu Rt$$

The solution of this equation is

$$x = A \sin \omega t + B \cos \omega t + \frac{\mu Rt}{c}$$

at $t = 0$, $x = 0$, $\dot{x} = 0$

$\therefore B = 0$

$$A = -\frac{\mu R}{\omega c}$$

then $x = -\frac{\mu R}{c}\left(\frac{1}{\omega} \sin \omega t - t\right)$

and $\dot{x} = \frac{\mu R}{c}(1 - \cos \omega t)$

If the drag force suddenly disappears at $t = t_s$, the equation of the second period is

$$m_2\ddot{x} + cx = 0$$

The solution of this differential equation is:

$$x = A \sin \omega t + B \cos \omega t$$

at $t = t_s$

$$x = x_{t_s} = \frac{\mu R}{c}\left(t_s - \frac{1}{\omega}\sin \omega t_s\right)$$

$$\dot{x} = \dot{x}_{t_s} = \frac{\mu R}{c}\left(1 - \cos \omega t_s\right)$$

If a new time ordinate $t^* = t - t_s$ instead of t,

at $t^* = 0$

$$B = \frac{\mu R}{c}\left(t_s - \frac{1}{\omega}\sin \omega t_s\right)$$

$$A = \frac{\mu R}{\omega c}\left(1 - \cos \omega t_s\right)$$

The elastic force is:

$$cx = c(A \sin \omega t^* + B \cos \omega t^*)$$

To obtain the best angle of inclination the following force equation results:

$$P_{z_t} = \sin \delta + (cx)_{max} \sin \delta = P_x \cos \delta$$

from which:

$$\tan \delta = \frac{P_x}{\left(1 + \frac{cx}{P_z}\right)P_z} = \frac{\mu}{\left(1 + \frac{cx}{P_z}\right)}$$

This method will now be used to calculate the optimum angle of suspension. Use will be made of experimental data collected from tests on the strut at zero angle of inclination.

The period of vibration of the cantilever spring system is taken at .15 seconds from Figure 7 of experimental data.

$T = .15$ sec.

$\omega = \frac{2\pi}{T} = 41.8$ rad/sec.

$t_s = .08$ sec. (time of complete rolling)

$\omega t_s = 192^\circ$

$\mu = .63$

$R = 42,000$

$\mu R = 26,400$

Using this data the following constants are calculated:

$A = \frac{1250}{c}$

$B = \frac{2210}{c}$

The elastic force is:

$cx = 1250 \sin\omega t^* + 2210 \cos\omega t^*$

This elastic force is a maximum at

$t^* = .0253$ sec.

$(cx)_{max} = 2360$

The vertical force occuring at this time is

$P_z t^* = Rt^* = 5250$

$$\tan\delta = \frac{.63}{1 - \frac{2360}{5250}}$$

The optimum angle becomes:

$\delta = 23^\circ - 31'$

D. Notation

z_1 = Displacement of m_1 in z - direction

z_2 = Displacement of m_2 in z - direction

m_1 = Half of airplane mass without masses of the wheel and the attached parts

m_2 = Masses of the wheel and the attached parts

k = Oleo spring constant

c = Oleo damping constant

k_1 = Oleo spring constant in z - direction

k_3 = Oleo spring constant in x - direction

k_2 = Tire spring constant

c_1 = Oleo damping constant in z - direction

c_2 = Oleo damping constant in x - direction

P_x = Force perpendicular to oleo axis, operating in the center of the wheel

P_{zt} = Spring force of the tire

V_s = Sinking velocity

V_L = Landing velocity

t = Time

r_t = Radius of tire

I_w = Moment of inertia of wheel with regard to the center

μ = Coefficient of friction

δ = Slope angle of the shock strut in comparison to the perpendicular of the ground

Θ = Wheel - spin angle

ω = Bending frequency of the cantilever strut assembly

BIBLIOGRAPHY

The Actual Loads On Airplane Landing Gear, by S. S. Shiskin, T.M. No. 821, N.A.C.A., 1937.

The Shock-Absorbing System of the Airplane Landing Gear, by P. Gallerio, T.M. No. 933, N.A.C.A., 1940.

Aircraft Wheel Inertia Drag Loads, T.S.E.L.A.-2B-4263-4, Aircraft Laboratory, Air Material Command.

Aircraft Wheel Inertia Drag Loads - Laboratory Investigation of Inertia Loads on B-24 Type Landing Gear, TSEAC9-4263-46-4, Add. 3, Aircraft Laboratory, Air Material Command.

Loads On And Behavior Of Landing Gears During The First Phase Of The Landing Impact, by W. Boccius; Technical Report F-TR-1172-ND, Aircraft Division, Intelligence Department, Air Material Command.